




ORIGINAL ARTICLE

KRAS-G12D mutation drives immune suppression and the primary resistance of anti-PD-1/PD-L1 immunotherapy in non-small cell lung cancer

Chengming Liu^{1,2} | Sufei Zheng^{1,2} | Zhanyu Wang^{1,2} | Sihui Wang^{1,2} |
 Xinfeng Wang^{1,2} | Lu Yang³ | Haiyan Xu⁴ | Zheng Cao⁵ | Xiaoli Feng⁵ |
 Qi Xue¹  | Yan Wang³  | Nan Sun^{1,2} | Jie He^{1,2} 

¹Department of Thoracic Surgery, National Cancer Center/National Clinical Research Center for Cancer/Cancer Hospital, Chinese Academy of Medical Sciences and Peking Union Medical College, Beijing 100021, P. R. China

²State Key Laboratory of Molecular Oncology, National Cancer Center/National Clinical Research Center for Cancer/Cancer Hospital, Chinese Academy of Medical Sciences and Peking Union Medical College, Beijing 100021, P. R. China

³Department of Medical Oncology, National Cancer Center/National Clinical Research Center for Cancer/Cancer Hospital, Chinese Academy of Medical Sciences and Peking Union Medical College, Beijing 100021, P. R. China

⁴Department of Comprehensive Oncology, National Cancer Center/National Clinical Research Center for Cancer/Cancer Hospital, Chinese Academy of Medical Sciences and Peking Union Medical College, Beijing 100021, P. R. China

⁵Department of Pathology, National Cancer Center/National Clinical Research Center for Cancer/Cancer Hospital, Chinese Academy of Medical Sciences and Peking Union Medical College, Beijing 100021, P. R. China

Correspondence

Jie He, Department of Thoracic Surgery, National Cancer Center/National Clinical Research Center for Cancer/Cancer Hospital, Chinese Academy of Medical Sciences and Peking Union Medical College, Beijing 100021, P. R. China.
 Email: prof.jiehe@gmail.com

Abstract

Background: Although immune checkpoint inhibitors (ICIs) against programmed cell death protein 1 (PD-1) and its ligand PD-L1 have demonstrated potency towards treating patients with non-small cell lung carcinoma (NSCLC), the potential association between Kirsten rat sarcoma viral oncogene homolog (*KRAS*) oncogene substitutions and the efficacy of ICIs remains unclear. In this

List of abbreviations: NSCLC, non-small cell lung cancer; LUAD, lung adenocarcinoma; LUSC, lung squamous cell carcinoma; *ALK*, anaplastic lymphoma kinase; *EGFR*, epidermal growth factor receptor; *KRAS*, Kirsten rat sarcoma viral oncogene homolog; ICIs, immune checkpoint inhibitors; PD-1, programmed cell death protein 1; PD-L1, programmed cell death-ligand 1; TIME, tumor immune microenvironment; TILs, tumor-infiltrating lymphocytes; TMB, tumor mutational burden; MAPK, mitogen-activated protein kinase; PI3K, phosphatidylinositol 3-kinase; CTLA-4, cytotoxic T-lymphocyte antigen 4; MSKCC, Memorial Sloan Kettering Cancer Center; CICAMS, Cancer Hospital and Institute, Chinese Academy of Medical Sciences; IHC, immunohistochemistry; BEGM, bronchial epithelial cell growth medium; FBS, fetal bovine serum; RT-qPCR, reverse transcription quantitative PCR; Erk1/2, extracellular signal-regulated kinase 1 and 2; HMGA2, high mobility group protein A2; CXCL10, chemokine (C-X-C motif) ligand 10; PBS, phosphate buffer saline; TPS, tumor proportion score; DAPI, 4',6-diamidino-2-phenylindole; ELISA, enzyme linked immunosorbent assay; PBMCs, peripheral blood mononuclear cells; PAM, protospacer adjacent motif; TCGA, The Cancer Genome Atlas; GO, Gene ontology; KEGG, Kyoto Encyclopedia of Genes and Genomes; TIMER, Tumor Immune Estimation Resource; PFS, progression-free survival; DCB, durable clinical benefit; mAb, monoclonal antibodies; *GZMB*, Granzyme B; mRNA, messenger RNA; mTOR, mechanistic target of rapamycin; PDO, patient-derived organoid; PD, progressive disease; OS, overall survival; TGF-beta, transcription of growth factor beta; EMT, epithelial-to-mesenchymal transition.

This is an open access article under the terms of the [Creative Commons Attribution-NonCommercial-NoDerivs](https://creativecommons.org/licenses/by-nc-nd/4.0/) License, which permits use and distribution in any medium, provided the original work is properly cited, the use is non-commercial and no modifications or adaptations are made.

© 2022 The Authors. *Cancer Communications* published by John Wiley & Sons Australia, Ltd. on behalf of Sun Yat-sen University Cancer Center.

Nan Sun, State Key Laboratory of Molecular Oncology, National Cancer Center/National Clinical Research Center for Cancer/Cancer Hospital, Chinese Academy of Medical Sciences and Peking Union Medical College, Beijing 100021, P. R. China.

Email: sunnan@vip.126.com

Funding information

National Natural Science Foundation of China, Grant/Award Numbers: 82072590, 81502514, 81802299; Graduate Innovation Funds of Peking Union Medical College, Grant/Award Number: 2019-1002-06; National Key Basic Research Development Plan, Grant/Award Number: 2018YFC1312105; National Key R&D Program of China, Grant/Award Numbers: 2018YFC1312100, 2018YFC1312102; Fundamental Research Funds for the Central Universities, Grant/Award Number: 3332018070; CAMS Innovation Fund for Medical Sciences, Grant/Award Numbers: 2016-12M-1-001, 2017-12M-1-005

study, we aimed to find point mutations in the *KRAS* gene resistant to ICIs and elucidate resistance mechanism.

Methods: The association between *KRAS* variant status and the efficacy of ICIs was explored with a clinical cohort ($n = 74$), and confirmed with a mouse model. In addition, the tumor immune microenvironment (TIME) of *KRAS*-mutant NSCLC, such as CD8⁺ tumor-infiltrating lymphocytes (TILs) and PD-L1 level, was investigated. Cell lines expressing classic *KRAS* substitutions were used to explore signaling pathway activation involved in the formation of TIME. Furthermore, interventions that improved TIME were developed to increase responsiveness to ICIs.

Results: We observed the inferior efficacy of ICIs in *KRAS*-G12D-mutant NSCLC. Based upon transcriptome data and immunostaining results from *KRAS*-mutant NSCLC, *KRAS*-G12D point mutation negatively correlated with PD-L1 level and secretion of chemokines CXCL10/CXCL11 that led to a decrease in CD8⁺ TILs, which in turn yielded an immunosuppressive TIME. The analysis of cell lines overexpressing classic *KRAS* substitutions further revealed that *KRAS*-G12D mutation suppressed PD-L1 level via the P70S6K/PI3K/AKT axis and reduced CXCL10/CXCL11 levels by down-regulating high mobility group protein A2 (HMGA2) level. Notably, paclitaxel, a chemotherapeutic agent, upregulated HMGA2 level, and in turn, stimulated the secretion of CXCL10/CXCL11. Moreover, PD-L1 blockade combined with paclitaxel significantly suppressed tumor growth compared with PD-L1 inhibitor monotherapy in a mouse model with *KRAS*-G12D-mutant lung adenocarcinoma. Further analyses revealed that the combined treatment significantly enhanced the recruitment of CD8⁺ TILs via the up-regulation of CXCL10/CXCL11 levels. Results of clinical study also revealed the superior efficacy of chemo-immunotherapy in patients with *KRAS*-G12D-mutant NSCLC compared with ICI monotherapy.

Conclusions: Our study elucidated the molecular mechanism by which *KRAS*-G12D mutation drives immunosuppression and enhances resistance of ICIs in NSCLC. Importantly, our findings demonstrate that ICIs in combination with chemotherapy may be more effective in patients with *KRAS*-G12D-mutant NSCLC.

KEYWORDS

KRAS-G12D, non-small cell lung carcinoma, immunotherapy, PD-L1, tumor-infiltrating lymphocyte, chemo-immunotherapy

1 | INTRODUCTION

Lung cancer, poses a serious threat to human health, as indicated by the top-ranking morbidity and mortality rates worldwide [1] and in China [2, 3]. Non-small cell lung cancer (NSCLC), including lung adenocarcinoma (LUAD) and lung squamous cell carcinoma (LUSC), accounts for ~85% of lung cancers in patients as the most common pathological subtype [4]. Nevertheless, more than 40% of

those diagnosed with NSCLC are already at stage IIIB or IV, whereby the best opportunity for surgical removal of the tumor has been missed [5]. Benefiting from the rapid development of medical molecular biology in the past decade, the therapies for metastatic or advanced NSCLC have transitioned from cytotoxic chemotherapy into the era of molecular targeted therapy [6]. For example, tyrosine kinase inhibitors against anaplastic lymphoma kinase (ALK) and epidermal growth factor receptor (EGFR) have

been extensively used as targeted therapies for NSCLC in the clinic [7–10]. In contrast, despite clinical studies on the small-molecule inhibitors AMG510 [11] and MRTX849 [12], targeting the Kirsten rat sarcoma viral oncogene homolog (*KRAS*) G12C mutation, most countries have no routinely used *KRAS*-targeted therapies [13].

In recent years, immune checkpoint inhibitors (ICIs) against programmed cell death protein 1 (PD-1) and its ligand programmed cell death-ligand 1 (PD-L1) have revolutionized the treatment paradigm of NSCLC and provided an approach for the treatment of refractory patients with NSCLC [14], particularly patients with *KRAS* mutations [15, 16]. Our previous publication [17] proved that patients with *KRAS*-mutant NSCLC have a superior response to ICIs due to an inflammatory tumor immune microenvironment (TIME) with adaptive immune resistance. However, only 58% of NSCLC patients with *KRAS*-mutant NSCLC were shown to have a high expression of PD-L1 and infiltration of CD8⁺ tumor-infiltrating lymphocytes (TILs), and not all patients benefited from anti-PD-1 immunotherapy. We speculated that the patients who presented with primary drug resistance might lack an inflammatory TIME. Therefore, exploration of the TIME in patients with *KRAS*-mutant NSCLC is needed to effectively distinguish responders from non-responders treated with ICIs. By changing the TIME, a greater proportion of the population could benefit from immunotherapy, thereby establishing a new treatment paradigm for patients with *KRAS*-mutant NSCLC.

KRAS is an important driver gene in the development of NSCLC, and the mutation rates of *KRAS* in Western [18] and Asian patients [19] with NSCLC are 20%-30% and 10%-15%, respectively. In NSCLC, *KRAS* oncogene substitutions often occur at codons 12 and 13 of exon 2, with common codon variants containing G12C (c.34G > T, 32.11%), G12D (c.35G > A, 23.39%), G12V (c.35G > T, 21.10%), and G12A (c.35G > C, 12.84%) [20, 21]. Of these substitutions, G12C, G12V and G12A are transversion mutations, while G12D is a transition mutation [22]. Notably, previous studies have shown that NSCLC with G12C, G12V, and G12A mutations are typical for smoking-related tumors with high tumor mutational burden (TMB), while the *KRAS*-G12D point mutation is an exception [23, 24]. In addition, several studies have shown that not all subtypes of *KRAS* mutations have similar biological effects. Subtype heterogeneity also exists with regards to the survival prognosis of patients [21] and the efficacy of chemotherapy [22], molecular targeted therapy [25] and immunotherapy [26]. As shown previously [27, 28], the GTPase activity of the *KRAS*-G12V point mutant protein is one-fourth that of the G12D point mutant protein, and one-tenth that of wild-type *KRAS*. Compared with the G12D point mutant protein, the G12V point mutant protein binds tighter to GTP. Consequently,

the G12V point mutant protein exists in a persistent spontaneous activated state. Furthermore, in addition to the mitogen-activated protein kinase (MAPK) signaling pathway, different substitutions of the *KRAS* oncogene activate various downstream signaling pathways. For example, the G12C and G12V mutations enhance the RalGDS-Ral pathway, while the G12D point mutations activates the phosphatidylinositol 3-kinase (PI3K)-AKT pathway [27]. In part, these mechanisms explain the disparities among the subtypes between the prognostic value and malignant transformation ability. Some recent studies have focused on the association between mutant variants of the *KRAS* gene and tumor immunity-related characteristics, including TMB, PD-L1 expression, and the presence of immune cells. However, the underlying association between *KRAS* oncogene substitutions and the efficacy of immunotherapy against PD-1/PD-L1 remains unclear, as does the mechanism of different substitutions, leading to immunotherapeutic heterogeneity [23, 29, 30].

In this study, the relationship between *KRAS* variant status and the efficacy of ICIs was investigated using an online clinical cohort, as well as cellular and mouse models. The immune landscapes, including CD8⁺ TILs, PD-L1, and immune-related genes levels, of patients with NSCLC harboring different substitutions of *KRAS* oncogene were analyzed, and the pathway activation involved in the formation of TIME was explored to find interventions with improved responsiveness to immunotherapy targeting PD-1/PD-L1.

2 | MATERIALS AND METHODS

2.1 | Clinical cohorts

To analyze the association between the *KRAS* variant status and efficacy of anti-PD-1/PD-L1 immunotherapy in NSCLC, the clinical data of 240 patients treated with anti-PD-1/PD-L1 alone or in combination with anti-cytotoxic T-lymphocyte antigen 4 (anti-CTLA-4) immunotherapy between April 2011 and January 2017 at the Memorial Sloan Kettering Cancer Center (MSKCC, New York, NY, USA) was downloaded from a previously published clinical cohort study [31]. According to the inclusion criteria (patients had *KRAS* mutations and received anti-PD-1/PD-L1 monotherapy) and exclusion criteria (patients with *EGFR* mutation), the clinical data of 74 patients who had *KRAS* mutations and received anti-PD-1/PD-L1 monotherapy was included in the analysis.

To investigate the clinical outcome of patients with NSCLC harboring *KRAS*-G12D mutations after initiation of PD-1/PD-L1 blockade monotherapy or chemotherapeutic immunotherapy, the clinical information of 11 NSCLC

patients who harbored *KRAS*-G12D mutations and received immunotherapy, with or without chemotherapy, at the Cancer Hospital and Institute, Chinese Academy of Medical Sciences (CICAMS, Beijing, China) was retrospectively collected between September 2017 and April 2021. The inclusion criteria were that patients had *KRAS*-G12D mutations and received ICIs; the exclusion criteria were that patients had *EGFR* mutation and received other treatments in addition to ICIs and chemotherapy. Of the 11 patients enrolled, 3 received anti-PD-1 agent monotherapy, and 8 received chemo-immunotherapy. The last follow-up time was June 15th, 2021.

A total of 112 *KRAS*-mutant NSCLC specimens surgically resected between January 2008 and December 2013 were collected from the biobank of CICAMS for immunohistochemistry (IHC) analysis. The inclusion criteria were that the tumor tissues were pathologically diagnosed as NSCLC with *KRAS* mutations; the exclusion criteria were that patients had *EGFR* mutation and received chemotherapy or radiotherapy before surgery. This study was approved by the Ethics Committee of CICAMS (approval number: #20/242-2438). The tissue samples were obtained with written informed consent from each patient.

2.2 | Cell lines and cell culture

Immortalized human bronchial epithelial cells (Beas-2B) were cultured in bronchial epithelial cell growth medium (BEGM) media (#CC-3170; Lonza, Basel, Switzerland) with 10% fetal bovine serum (FBS, #35-081-CV; Corning, New York, NY, USA). Human lung cancer cell lines (Calu3, H1703, H2030, H358, SK-LU-1, A427, H441, H292, A549, and H460) were cultured in RPMI-1640 media (#10-040-CV; Corning) containing 10% FBS and antibiotic mixture (100 U/mL penicillin and 100 µg/mL streptomycin, #15140-122; Gibco, Billings, MT, USA). H2009 and 293T cells were cultured in Dulbecco's modified eagle medium (DMEM) media (#10-013-CVR; Corning) containing 10% FBS and antibiotic mixture. LA795 cells (clones from the lungs of a 615 mouse with LUAD) were cultured in RPMI-1640 media containing 10% FBS and an antibiotic mixture.

2.3 | Reverse transcription quantitative PCR (RT-qPCR), Western blotting, flow cytometry, IHC, and immunofluorescence

RT-qPCR, Western blotting, flow cytometry and IHC were performed as previously described [17, 32, 33]. Total RNA was extracted with TRIzol reagent (#15596; Life Technologies, Carlsbad, CA, USA). TransScript[®] II All-in-One First-Strand cDNA Synthesis SuperMix kit (#AH341-01;

TransGen, Beijing, China) was used for reverse transcription. RT-qPCR was performed with TransStart[®] Top Green qPCR SuperMix (#AQ132; TransGen) on ABI 7900HT Real-Time PCR thermocycler (Life Technologies). The human and mouse PCR primers used in this study are shown in Supplementary Tables S1 and Supplementary Tables S2, respectively.

The primary antibodies for Western blotting used in this study are listed as follows: PD-L1 (#13684T; Cell Signaling Technology, Danvers, MA, USA), *KRAS* (#3339T; Cell Signaling Technology), *KRAS* G12D (#14429S; Cell Signaling Technology), β -Tubulin (#2128T; Cell Signaling Technology), Flag (#F3165; Sigma-Aldrich, Saint Louis, MO, USA), GAPDH (#ab8245; Abcam, Cambridge, UK), extracellular signal-regulated kinase 1 and 2 (Erk1/2, #4695; Cell Signaling Technology), Phospho-Erk1/2 (Thr202/Tyr204) (#4370; Cell Signaling Technology), AKT (#4691; Cell Signaling Technology), Phospho-AKT (Ser473) (#4060; Cell Signaling Technology), Phospho-AKT (Thr308) (#13038; Cell Signaling Technology), p70S6K (#2708; Cell Signaling Technology), phospho-p70S6K (Thr389) (#9234; Cell Signaling Technology), p70S6K (#66638-1-Ig; Proteintech, Rosemont, IL, USA), high mobility group protein A2 (HMGA2; #8179S; Cell Signaling Technology), chemokine (C-X-C motif) ligand 10 (CXCL10, #ab137018; Abcam), CXCL11 (#MAB672-SP; R&D, Minneapolis, MN, USA) and Actin (#66009-1-Ig; Proteintech). Briefly, cell protein lysates were electrophoresed using PAGE Gel Quick Preparation Kit (#8012011; Dakewe, Shenzhen, Guangdong, China) and transferred to PVDF membranes (#P2120-2; APPLYPGEN, Beijing, China). After incubation with the primary antibodies at 4°C overnight, the membranes with HRP (horseradish peroxidase)-conjugated secondary antibodies at room temperature for 1 h. Finally, we visualized the protein bands using enhanced chemiluminescence.

The antibodies for flow cytometry used in this study included PD-L1 (APC, #329707; BioLegend, San Diego, CA, USA) and its isotype control (APC, #401210; BioLegend). Briefly, the antibodies were used to incubate cells at 4°C for 30 min. Phosphate buffer saline (PBS, #D8537; Sigma-Aldrich) was then used to wash and suspend cells for flow cytometric analysis.

The primary antibodies for IHC used in this study are listed as follows: PD-L1 (SP263 clone, #740-4907; Ventana Medical Systems, Oro Valley, AZ, USA), CD8 (#ZA-0508; Zsbio Tech, Beijing, China), HMGA2 (#8179S; Cell Signaling Technology), CXCL10 (#MAB2662-SP; R&D), CXCL11 (#MAB672-SP; R&D), PD-L1 (#ab238697; Abcam), CD8 (#98941; Cell Signaling Technology), CXCL10 (#10937-1-AP; Proteintech) and CXCL11 (#MAB572-SP; R&D). Briefly, the tumor tissue sections were incubated with these primary antibodies at 4°C overnight and then incubated with HRP-conjugated secondary antibodies at 25°C

for 1 h after antigen retrieval. The PD-L1 tumor proportion score (TPS) and the proportion of CD8⁺ T cells were assessed according to the evaluation criteria of the previously published approach [17]. The IHC score was calculated using the following formula: IHC score = staining intensity × percentage of positive tumor cells × 100. There are four grades of staining intensity: no color staining was recorded as 0, pale yellow staining as 1, yellow staining as 2, and brown-yellow staining as 3 [34].

The primary antibodies for immunofluorescence used in this study included CD86 (#GB13585; Servicebio, Wuhan, Hubei, China) and CD11c (#GB11059; Servicebio). Briefly, the tumor tissue sections were incubated with these primary antibodies at 4°C overnight, and then stained with 4',6-diamidino-2-phenylindole (DAPI, #28718-90-3; Beyotime, Shanghai, China) to label nuclei for 15 min. Next, the sections were probed with secondary antibodies with fluorescence according to the primary antibodies used.

2.4 | Cell supernatant extraction and enzyme-linked immunosorbent assay (ELISA)

Cell supernatant extraction and ELISA were performed as previously described [32]. The concentration of free CXCL10 and CXCL11 protein in extracted cell supernatants was detected by the Human CXCL10/IP-10 Quantikine ELISA Kit (#DIP100; R&D) and the Human CXCL11/I-TAC Quantikine ELISA Kit (#DCX110; R&D) according to the manufacturer's instructions.

2.5 | In vitro tumoricidal activity assays

Human peripheral blood mononuclear cells (PBMCs) were obtained from peripheral blood provided by healthy donors using Ficoll Paque Plus density centrifugation (#17-1440-02; GE Healthcare, Cleveland, OH, USA). We then used the Human CD8⁺ T Cell Isolation kit (#130-096-495; Miltenyi Biotec, Bergisch Gladbach, Germany) to isolate CD8⁺ T cells from the PBMCs, and cultured the isolated CD8⁺ T cells in RPMI-1640 media containing 10% FBS, 200 U/mL interleukin-2 (IL-2, #200-02-50; PeproTech, Rocky Hill, NJ, USA) and an antibiotic mixture. Meanwhile, we added human anti-CD3/CD28 Dynabeads (#40203D; Thermo Fisher Scientific, Waltham, MA, USA) in the media to activate CD8⁺ T cells for 3 days based on the manufacturer's protocol. After A427, SK-LU-1, H2009, H358 and H441 cells adhered to the plate overnight, we co-cultured tumor cells and activated CD8⁺ T cells in a ratio of 1:5 for 48 h in the presence of isotype control or nivolumab (200 µg/mL, #A2002; Selleck, Shanghai, China). Next, we used the Cell Counting Kit-8 (#CK04;

Dojindo, Kumamoto, Japan) to quantify living tumor cells after removing T cells and cellular debris.

2.6 | Construction of *KRAS*-knockout cells

We first designed the single-guide RNA (3'-CTGAATTAGCTGTATCGTCA-5') for mice and single-guide RNA (5'-CAATGAGGGACCAGTACATG-3') for human using DeepCRISPR [35]. For single-guide RNA cloning, the SpCas9 targeting vector (#H11761; OBiO, Shanghai, China) was then digested with BsmBI (#ER0451; Thermo Fisher Scientific) and ligated with BsmBI-compatible annealed oligos (OBiO). We harvested lentiviruses using 293T cells as previously described [36]. Briefly, 293T cells were co-transfected with the SpCas9 targeting vector and packaging plasmid (pLP1, pLP2, and pLP/VSVG; OBiO) using Lipofectamine 3000 (#L3000015; Invitrogen, Carlsbad, CA, USA). We harvested the infectious lentiviruses at 48 h after transfection. LA795 and Beas-2B cells were then infected with harvested lentiviruses by the addition of 6 µg/mL polybrene (#P4505; Sigma-Aldrich), and single-cell clones were selected with mCherry using flow cytometry sorting. The knockout effect of *KRAS* in the infected cells was confirmed by Western blotting and Sanger sequencing after selection.

2.7 | Construction of stable *KRAS*-overexpressing cells

For stable overexpression of exogenous *KRAS* plasmids, coding for wild-type *KRAS* (WT), mutant *KRAS*-Gly12Ala (G12A), mutant *KRAS*-Gly12Cys (G12C), mutant *KRAS*-Gly12Asp (G12D), or mutant *KRAS*-Gly12Val (G12V), cDNA was ligated into the lentiviral vector (mouse: #H11219; human: #GL122; OBiO). It is worth noting that the protospacer adjacent motif (PAM) region of single-guide RNA needs synonymous mutation in the cDNA. According to the above-mentioned methods of lentivirus production and infection, we gained the infected cells. Infected single-cell clones were then selected with EGFP using flow cytometry sorting. Western blotting was performed to determine the efficiency of the overexpression.

2.8 | In vivo mouse experiments

Female mice (specific pathogen-free, 5-6 weeks old) were used for the animal experiments. The mice were purchased from the Institute of Hematology, Chinese Academy of Medical School (Tianjin, China) and housed at the Center of Experimental Animals of CICAMS. The Animal Care

and Use Committee of CICAMS approved all procedures concerning in vivo mouse experiments (approval number: #NCC2020A163).

A total of 615 mice were subcutaneously implanted with murine LA795-derived xenografts that harbored different *KRAS* oncogene substitutions, including G12A, G12C, G12D and G12V, and treated with anti-PD-L1 monoclonal antibody (10 mg/kg three times weekly; Bio X Cell, West Lebanon, NH, USA) or paclitaxel (20 mg/kg twice weekly; CSPC, Shijiazhuang, Hebei, China) when the tumor volume reached $\sim 100 \text{ mm}^3$. After the treatment intervention, all mice were euthanized by carbon dioxide asphyxiation to dissect the subcutaneous tumor for IHC analysis.

2.9 | Transcriptome sequencing data, immune cell infiltration analysis and TMB calculation

HTseq-Counts data of 139 LUAD samples with *KRAS* mutations were extracted from The Cancer Genome Atlas (TCGA) database (<https://portal.gdc.cancer.gov/>) and divided into two groups with or without *KRAS*-G12D mutations. We previously identified 1,584 genes that were differentially expressed between the two groups at the thresholds of $P < 0.05$ and $\log_2(\text{fold-change}) > 1$ using the “DESeq2” R package [37]. Finally, 39 out of 730 immune-related genes extracted from the nCounter PanCancer Immune Profiling Panel (NanoString) [38] were identified. Gene Ontology (GO) and Kyoto Encyclopedia of Genes and Genomes (KEGG) enrichment analyses were performed to determine the biological function and pathway correlated with the 39 differentially expressed genes in the DAVID 6.8 (<http://david.abcc.ncifcrf.gov>).

The Tumor Immune Estimation Resource (TIMER; <https://timer.cistrome.org>) was used to calculate the fractions of six intra-tumoral immune cells in each sample, according to the gene expression profile data. Notably, quantile-normalization method was used to standardize the gene expression profile data to eliminate the influence of confounding variables [39].

Somatic mutation data of LUAD were downloaded from the MSKCC dataset (<https://www.cbioportal.org/>) and TCGA database. By counting the total count of somatic mutations detected in the coding region, except silent mutations, TMB was calculated for each tumor sample.

2.10 | Organoid culture

LUAD samples with *KRAS*-G12D mutations were obtained from the CICAMS and were transported directly to the

laboratory after the surgery was performed. The patients provided informed consent. The study was approved by the Ethics Committee of the CICAMS (approval number: #20/242-2438). The tumor samples were washed twice with cold PBS and minced into smaller pieces using scissors. The protocol for establishing organoids was previously described [40]. Organoids were cultured in OrganoPro™ Tumor Organoids Culture Media (#K2O-M-NSCLC; Ketu Tech, Beijing, China), and passaged at a 1:3 ratio every 2-3 weeks.

2.11 | Statistical analysis

SPSS v21.0 (SPSS, Chicago, IL, USA) and Prism v8.0 (GraphPad, San Diego, CA, USA) was used for data analysis. The experimental data are expressed as the mean \pm standard deviation, and the data analysis between groups was conducted with Mann-Whitney *U* tests, one-way analysis of variance, and Student's *t*-test. Pearson correlation analysis was used to assess the association between samples. We used the Kaplan-Meier method to generate survival curves, and performed comparisons between groups by log-rank tests. *P* values less than 0.05 were considered statistically significant. The graphical abstract was created with BioRender.com. Based on the ARRIVE1 guidelines, we have completed the reporting checklist for study.

3 | RESULTS

3.1 | *KRAS*-G12D mutation was correlated with the primary resistance of ICI monotherapy in NSCLC

A clinical cohort of 74 NSCLC patients that harbored *KRAS* mutations and received anti-PD-1/PD-L1 monotherapy was enrolled to explore the correlation between *KRAS* variant status and the clinical benefit of ICIs (Supplementary Table S3). Depending on the variant status of the *KRAS* oncogene, these patients were assigned to five subgroups: G12A ($n = 7$), G12C ($n = 30$), G12D ($n = 11$), G12V ($n = 12$), and others ($n = 14$). As shown in Figure 1A, there were significant differences among the Kaplan-Meier survival curves of these five subgroups ($P = 0.044$). Notably, the NSCLC patients with *KRAS*-G12D mutations had significantly shorter progression-free survival (PFS) than those with other point mutations ($P = 0.006$; Figure 1B). Although the effect of immunotherapy is slow when compared with conventional anti-tumor therapy, a durable clinical benefit (DCB, PFS > 6 months) can often be obtained [15]. Differences were found among

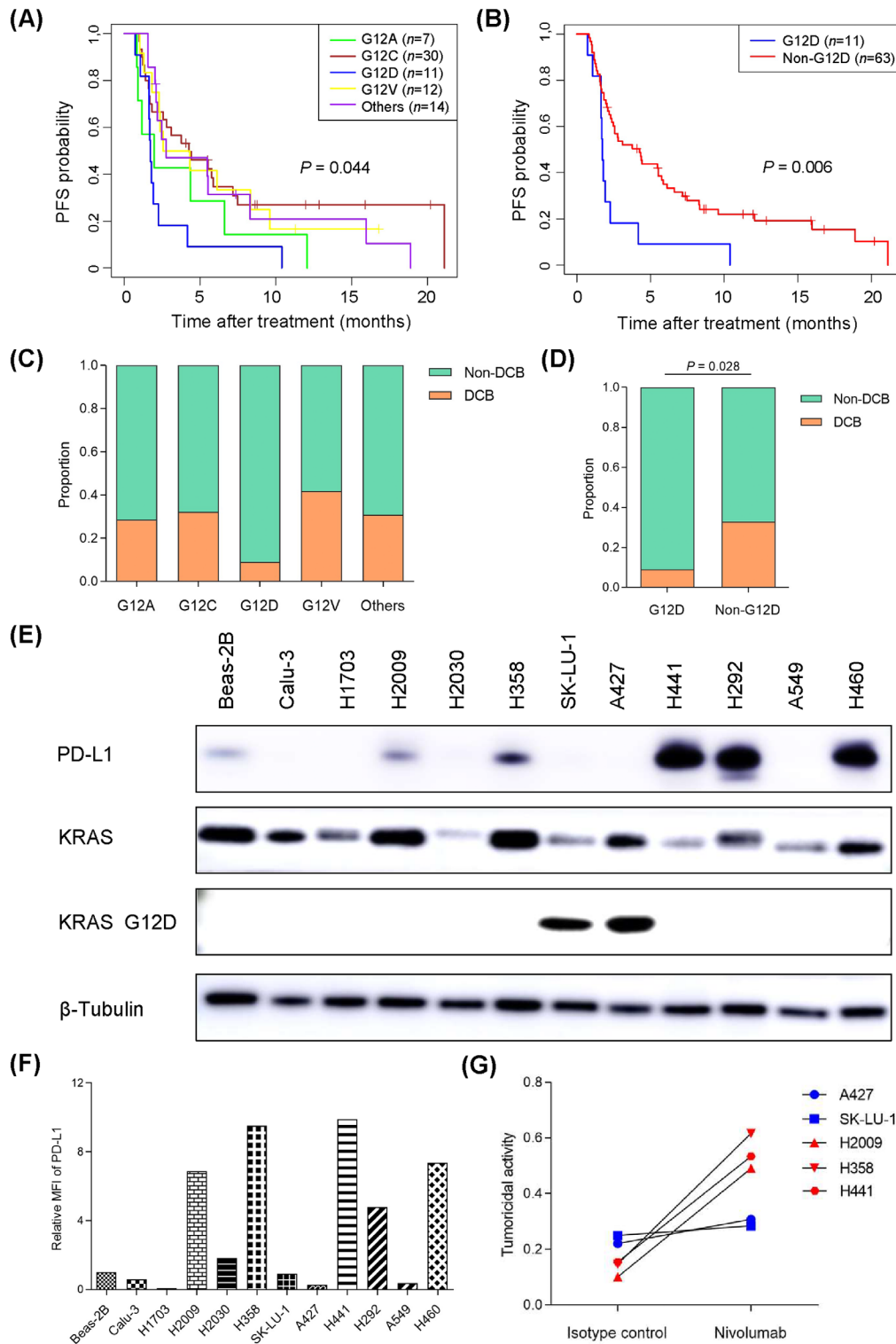


FIGURE 1 Relationships of *KRAS* oncogene substitutions with the efficacy of immunotherapy in NSCLC. (A) Kaplan-Meier survival curves of patients with NSCLC receiving anti-PD-1 monotherapy based on different subtypes of *KRAS* mutations concerning PFS. (B) Kaplan-Meier survival curves of patients with NSCLC receiving anti-PD-1 monotherapy between the two subgroups (G12D and non-G12D) concerning PFS. (C) Boxplots evaluating DCB of patients with NSCLC harboring different substitutions of *KRAS* mutations after anti-PD-1 monotherapy. (D) Boxplots evaluating DCB of patients with NSCLC between the two subgroups (G12D mutation and non-G12D mutations). (E-F) Western blotting (E) and flow cytometry (F) analysis of PD-L1 protein level in normal lung cell line and NSCLC cell lines. (G) The tumoricidal activity of CD8⁺ T cells cocultured with five NSCLC cell lines harboring *KRAS* mutations after treatment with isotype control and nivolumab (200 μg/mL) for 48 h (The blue marker indicates the cells with *KRAS*-G12D mutation, and the red indicates the cells without *KRAS*-G12D mutation). Abbreviations: G12D, samples with *KRAS*-G12D mutation; non-G12D, samples without *KRAS*-G12D mutation; DCB, patients with durable clinical benefit; non-DCB, patients without durable clinical benefit; PFS, progression-free survival.

groups when analyzing the DCB of patients with different substitutions (Figure 1C). Of note, the proportion of patients achieved DCB was lower in the G12D group than in the non-G12D group ($P = 0.028$; Figure 1D). By investigating the relationships between *KRAS* oncogene substitution and TMB in these patients, the results showed that patients with *KRAS*-G12D mutations exerted the lowest TMB (Supplementary Figure S1A-B). This finding was also verified using mutation data from the TCGA database (Supplementary Figure S1C).

To further confirm the clinical findings, a co-cultured system consisting of cytotoxic CD8⁺ T lymphocytes and tumor cells was established to evaluate the tumoricidal activity of CD8⁺ T cells cocultured with tumor cells harboring different *KRAS* oncogene substitutions (Supplementary Table S4). Western blotting and flow cytometry were firstly performed to detect the protein level of PD-L1 in Beas-2B cells and 11 NSCLC cell lines. The results showed that cell lines with *KRAS*-G12D mutation (A427 and SK-LU-1) had a lower level of PD-L1 than the other cell lines without *KRAS*-G12D mutation (Figure 1E-F). Of note, the tumoricidal activity of CD8⁺ T cells cocultured with the cell lines harboring non-G12D mutations increased significantly after nivolumab intervention; yet the cells carrying G12D mutations did not (Figure 1G).

In addition to the co-culture model, a mouse model was established to evaluate the efficacy of anti-PD-L1 drugs. We first knocked out the *KRAS* gene in LA795 cells without *KRAS* mutation, and then transferred lentivirus vectors coding four common *KRAS* oncogene substitutions (G12A, G12C, G12D and G12V) in *KRAS*-knockout LA795 cells (Supplementary Figure S2A-C). A previous study reported that *KRAS* mutations at different sites did not affect cell growth [27]. To further explore whether *KRAS* mutations at different sites affect the growth of subcutaneous tumors in mice, we subcutaneously transplanted LA795 cells carrying different *KRAS* substitutions into nude mice. It was found that there was no significant difference in the growth of subcutaneous tumors in these groups (Supplementary Figure S2D-E). Next, mice loaded with different *KRAS* point mutations were established by subcutaneously transplanting tumor xenografts derived from mouse LA795 cell lines carrying different *KRAS* substitutions into 615 mice (Figure 2A). Consistent with our findings in the clinical cohorts, anti-PD-L1 monoclonal antibodies (mAb) in mice with G12D mutations were less effective against tumor growth compared to other groups ($P < 0.001$; Figure 2B). Furthermore, from IHC analysis, there was a lower protein level of PD-L1 and less CD8⁺ T cell infiltration in mouse tumor specimens carrying the *KRAS*-G12D point mutation before the intervention of anti-PD-L1 antibodies compared to the other groups. In

contrast, after anti-PD-L1 antibody intervention, the mice in the G12D group did not show a markedly decreased PD-L1 protein level and increased CD8⁺ T cell infiltration as did the other groups (Figure 2C-D). In addition, results of immunofluorescence revealed that there was no significant difference in the number of activated CD86⁺ CD11c⁺ dendritic cells among these groups before the intervention of anti-PD-L1 antibodies, whereas the number of these cells in each group increased after anti-PD-L1 antibody intervention (Supplementary Figure S3).

3.2 | *KRAS*-G12D mutation contributed to an immune-suppressive TIME

Based upon 112 resected NSCLC samples with *KRAS* mutations (Supplementary Table S5), lower proportions of cells positive for PD-L1 protein expression and CD8⁺ T cell infiltration was observed in the G12D group compared with the non-G12D group (PD-L1: $P = 0.003$; CD8⁺ T cell: $P = 0.043$; Figure 3A-B). When the TIME was classified according to the PD-L1 status and the presence or absence of TILs [41, 42], significantly higher proportions of the TIME state with PD-L1-negative and no TILs was found in the G12D group ($P = 0.009$; Figure 3C), suggesting an immune-ignorance TIME in NSCLC samples with *KRAS*-G12D mutations.

To explore the underlying mechanism of immunosuppressive TIME induced by the *KRAS*-G12D mutation, we analyzed the gene expression profile of 139 LUAD samples with *KRAS* mutations from the TCGA database. Among 1584 genes differentially expressed in LUAD specimens with or without G12D mutations, 39 immune genes were determined (Figure 3D-E). We then performed GO and KEGG enrichment analysis to determine the biological function and pathway correlating with the 39 differentially expressed genes. The results showed that these genes were enriched in the leukocyte chemotaxis pathway, leukocyte migration pathway, and cytokine-cytokine receptor interaction pathway (Figure 3F-G). Looking for differential genes related to adaptive immune response, significantly lower expression of genes related to effector T cell activation and killing tumor cells, including *CD274*, *CXCL10*, *CXCL11* and Granzyme B (*GZMB*), were observed in the G12D group than in the non-G12D group (Figure 3H). *CXCL10* and *CXCL11*, as chemokines, are involved in the recruitment of CD8⁺ T cells into tumor tissues, thereby resulting in the killing of tumor cells [43]. IHC analysis of the protein levels of *CXCL10* and *CXCL11* in the 112 resected NSCLC samples with *KRAS* mutations confirmed that the G12D group showed lower levels of *CXCL10* and *CXCL11* than the non-G12D group (*CXCL10*: $P < 0.001$; *CXCL11*: $P = 0.001$; Figure 3I).

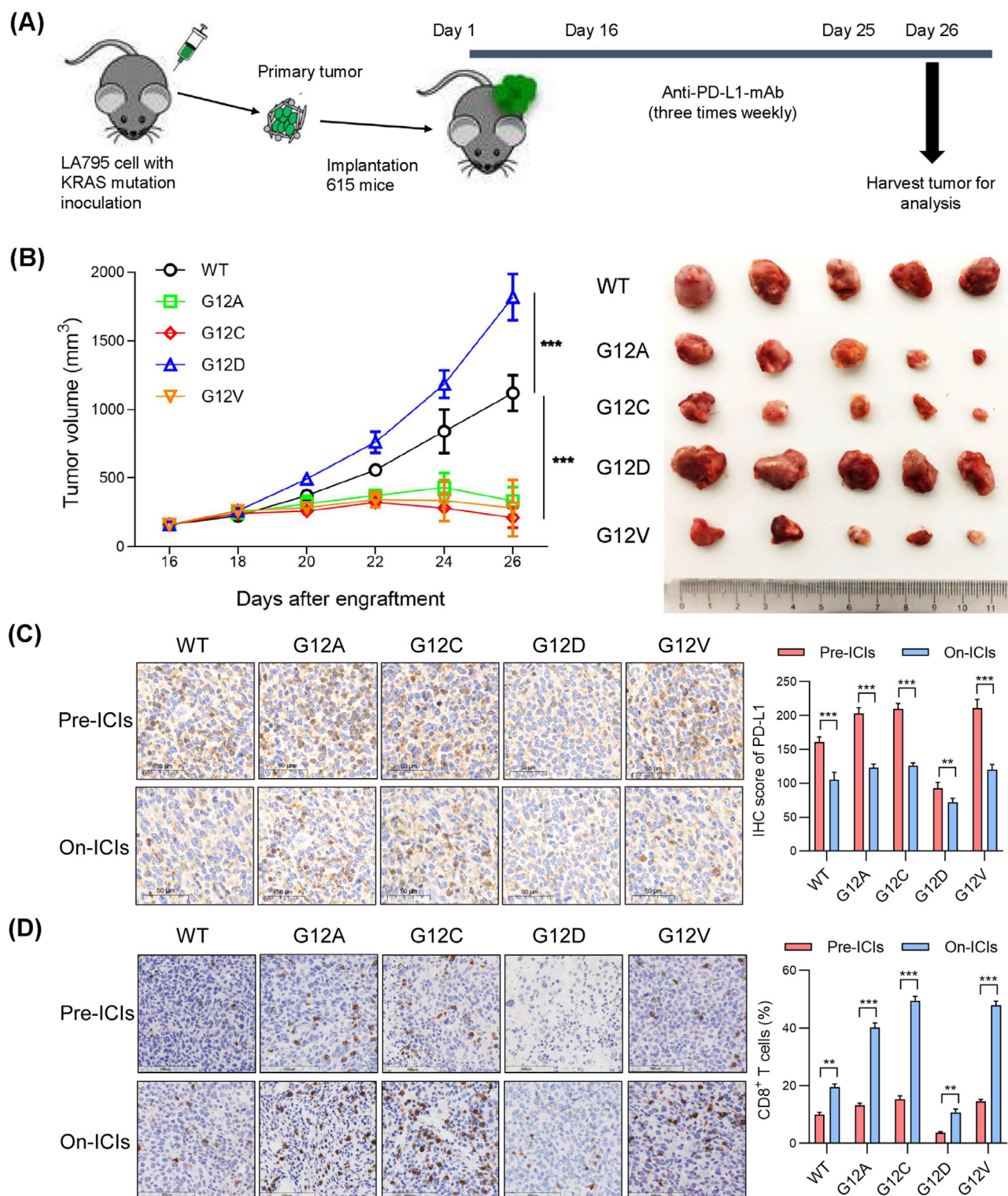


FIGURE 2 Mouse models to study the association between PD-L1 blockade efficacy and KRAS oncogene substitutions. (A) Scheme for constructing the mouse model with different subtypes of KRAS mutations and the dosing schedule. (B) The mice bearing LA795 cells with different subtypes of KRAS mutations received anti-PD-L1 monoclonal antibody (mAb) treatment. Anti-PD-L1 mAb did not reduce tumor growth significantly in the mice with KRAS-G12D mutation compared to other subtypes of KRAS mutations (left lane). Representative images of tumor nodules in each treated group (right lane). (C–D) The distributions of IHC score of PD-L1 level (C) and CD8⁺ T cells (D) in each treated group from B before and after PD-L1 blockade, as well as the representative immunohistochemistry images. **, $P < 0.01$; ***, $P < 0.001$. Abbreviations: WT, mice without KRAS mutation; G12A, mice with KRAS-G12A mutation; G12C, mice with KRAS-G12C mutation; G12D, mice with KRAS-G12D mutation; G12V, mice with KRAS-G12V mutation; Pre-ICIs, before using anti-PD-L1 monoclonal antibody; On-ICIs, after using anti-PD-L1 monoclonal antibody; IHC, immunohistochemistry.

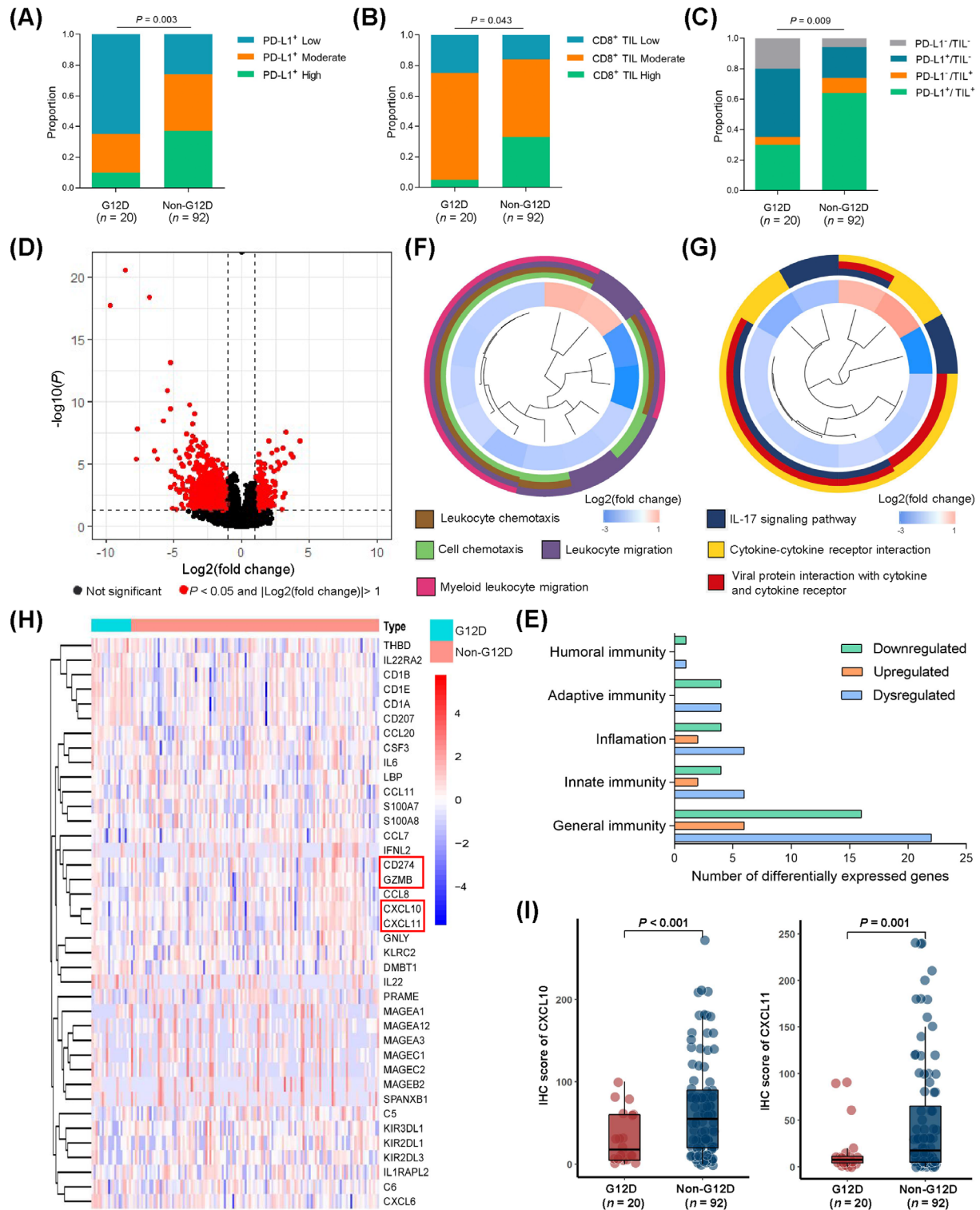


FIGURE 3 Tumor microenvironment and transcriptome data of KRAS-mutant NSCLC patients with or without KRAS-G12D point mutation. (A-C) IHC analysis of PD-L1 level (A), CD8⁺ TILs (B), and tumor microenvironment based on PD-L1 and CD8⁺ TILs (C) according to KRAS oncogene substitutions in a cohort of 112 NSCLC specimens with KRAS mutations. (D) Volcano plot of significantly down- and up-regulated genes in LUAD samples with KRAS-G12D mutation. (E) The distributions of remarkably dysregulated immune-related genes among the five classes based on immune response. (F-G) GO analysis (F) and KEGG analysis (G) of the biological pathways enriched for significantly dysregulated immune-related genes. (H) Heatmap plot of significantly dysregulated immune-related genes. (I) IHC analysis of protein levels of CXCL10 and CXCL11 in LUAD samples with or without KRAS-G12D mutation. Abbreviations: G12D, samples with KRAS-G12D mutation; non-G12D, samples without KRAS-G12D mutation; TIL, tumor infiltrating lymphocyte; GO, Gene ontology; KEGG, Kyoto Encyclopedia of Genes and Genomes; IHC, immunohistochemistry.

3.3 | *KRAS*-G12D mutation suppressed the infiltration of CD8⁺ T cells by regulating the *HMGA2*-*CXCL10*/*CXCL11* axis

To explore the molecular mechanism by which the *KRAS* mutation regulates differential expression of *CXCL10* and *CXCL11* in the tumor microenvironment, we first planned to knock out the *KRAS* gene in Beas-2B cells which express wild-type *KRAS* gene (Figure 4A). However, only single-cell clones with heterozygous *KRAS* gene knock-out survived (Figure 4B). Beas-2B cells with heterozygous *KRAS* gene knockout were then used to stably overexpress four common *KRAS* oncogene substitutions (Figure 4C). Of note, KEGG analysis of the biological processes and pathways enriched for the differential genes between the G12D-mutant and non-G12D-mutant cells suggested the involvement of cytokine-cytokine receptor interaction (Figure 4D). Next, we looked for the same significantly dysregulated genes between the LUAD samples and cell lines when comparing LUAD with *KRAS*-G12D mutations with other types of *KRAS* mutations, and identified 4 upregulated genes and 10 downregulated genes (Figure 4E-F). Then, a cross-correlogram was generated based on Pearson's correlation coefficient values among levels of PD-L1, *CXCL10*, *CXCL11* and 14 significantly dysregulated genes in the LUAD samples with *KRAS* mutations. A markedly positive relationship between the *HMGA2* level and that of PD-L1, *CXCL10* and *CXCL11* was found (Figure 4G). Considering that immune response is closely associated with the immune cell landscape, a TIMER algorithm was applied to analyze the relationship of *HMGA2* level with the intra-tumoral immune cell composition. *HMGA2* expression was positively related to the infiltration level of CD8⁺ T cells, neutrophils, myeloid dendritic cells and macrophages (Figure 4H). Furthermore, a positive correlation was confirmed through a combined analysis of the levels of *HMGA2*, PD-L1, *CXCL10* and *CXCL11* and the infiltration of CD8⁺ T cells in the IHC-detected group consisting of 112 resected NSCLC samples (Figure 4I). The IHC results of tumor tissues also demonstrated that the *KRAS*-G12D mutation induced low level of *HMGA2* compared to the other mutations ($P < 0.001$; Figure 4J). Consistent with the IHC results obtained from tumor tissues, Western blotting and RT-qPCR in cells with four common *KRAS* oncogene substitutions further confirmed that the *KRAS*-G12D mutation led to low levels of *HMGA2*, *CXCL10*, *CXCL11* and PD-L1 compared to other mutations (Figure 4K, Supplementary Figure S4A-D). The ELISA results also showed that *KRAS*-G12D mutation resulted in low secretion of *CXCL10* and *CXCL11* (Supplementary Figure S4E-F).

To verify the regulation mechanism between *HMGA2*, PD-L1, *CXCL10* and *CXCL11* levels, *HMGA2*-overexpressing Beas-2B-G12D, SK-LU-1, and A427 cell lines were analyzed. As speculated, *HMGA2* expression, whether at the protein or messenger RNA (mRNA) level, upregulated levels of *CXCL10* and *CXCL11*. *HMGA2* expression also increased levels of secreted *CXCL10* and *CXCL11*. Curiously, the level of PD-L1 was not regulated by *HMGA2* expression (Figure 4L, Supplementary Figure S5).

3.4 | *KRAS*-G12D mutation suppressed PD-L1 expression level via the P70S6K/PI3K/AKT axis

Previous studies have demonstrated that *KRAS* mutation stabilizes PD-L1 mRNA via the MEK-ERK signaling pathway [44]. However, a study reported that in addition to the MEK-ERK pathway, NSCLC cell lines with *KRAS*-G12D mutations had the activated PI3K-AKT pathway, whereas NSCLC cell lines with *KRAS*-G12V and *KRAS*-G12C mutations had the activated RalGDS-Ral pathway and the weakened activation of the PI3K-AKT pathway [27]. Hence, we speculated that different substitutions of the *KRAS* oncogene might differentially regulate PD-L1 level via the activation of different downstream signaling pathways.

Consistent with the previous study, *KRAS* mutation, regardless of the type of variation, promoted the phosphorylation of Erk1/2. However, compared to G12A, G12C and G12V point mutations, G12D point mutation activated the phosphorylation of AKT and reduced the phosphorylation of p70S6K (Figure 5A). These findings were also confirmed in LA795 cells with different substitutions of the *KRAS* oncogene (Supplementary Figure S6). Given that mechanistic target of rapamycin (mTOR) activation leads to feedback repression of the PI3K-AKT pathway through the effector p70S6K [45], *KRAS*-transfected Beas-2B cell lines were treated with the mTOR inhibitor (rapamycin, 0.5 $\mu\text{mol/L}$) for 24h, and the impact on the levels of PD-L1, *HMGA2*, *CXCL10* and *CXCL11*, as well as the downstream signaling, were investigated. Rapamycin induced activation of the AKT pathway in Beas-2B cells expressing G12A, G12C and G12V point mutations. However, in Beas-2B cells expressing the G12D point mutation, the AKT pathway was constitutively activated, and rapamycin did not further increase the phosphorylation of AKT (Figure 5B). In addition, regardless of the type of *KRAS* variation, PD-L1 levels were reduced to a consistent level under the intervention of rapamycin (Figure 5B, Supplementary Figure S7A). However, after the intervention of rapamycin, the

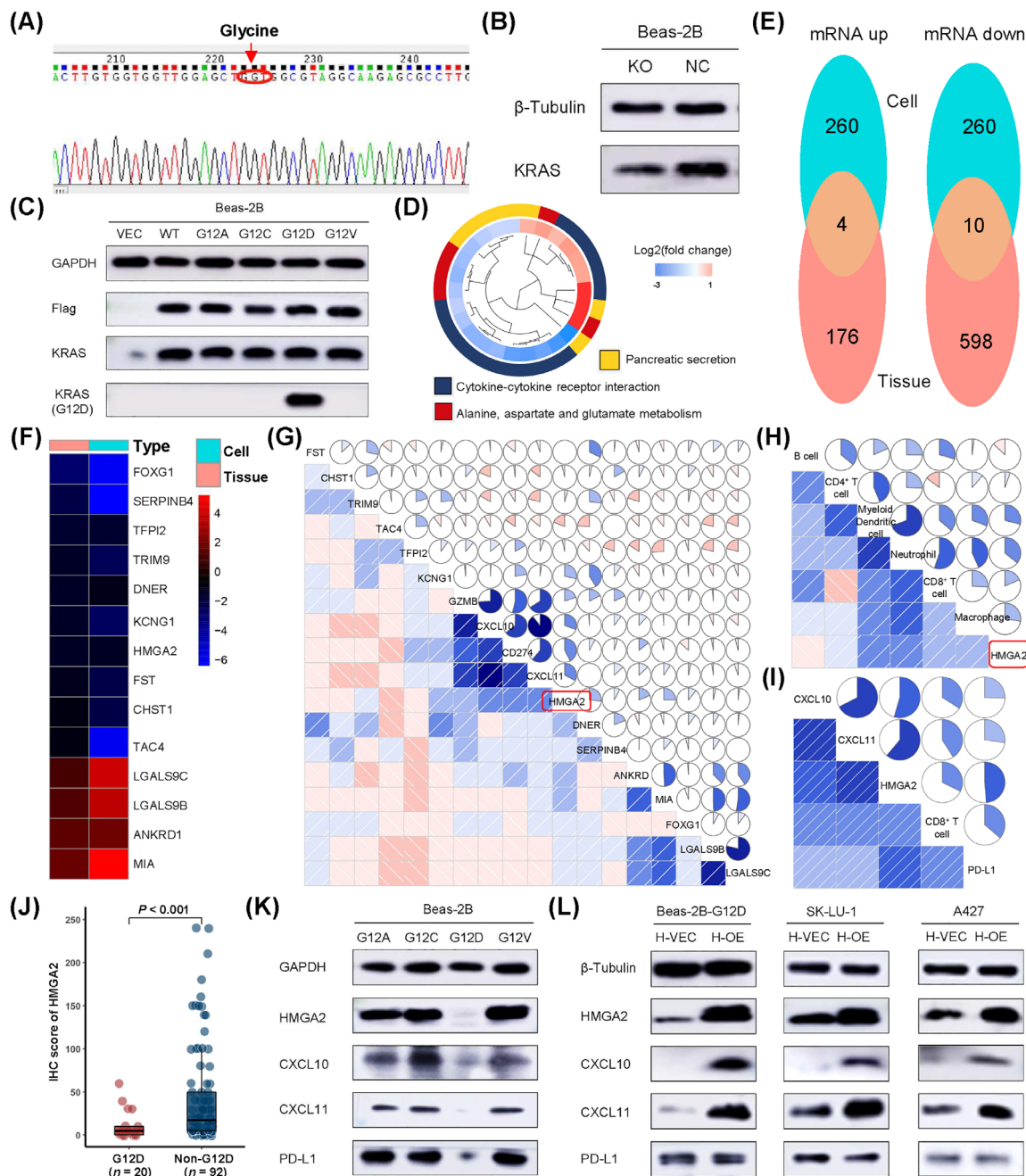


FIGURE 4 Down-regulation of PD-L1, CXCL10, CXCL11, and HMGA2 levels in LUAD samples with KRAS-G12D mutation. (A) The sequence of Beas-2B cells confirmed the presence of wild-type KRAS gene. (B) Western blotting analyzed the KRAS protein level in Beas-2B cells with heterozygous KRAS gene knockout. (C) Western blotting analysis of flag, KRAS, and KRAS-G12D protein levels in Beas-2B cells stably transfected with empty vector (VEC), vector coding for wild-type KRAS (WT), mutant KRAS-Gly12Ala (G12A), mutant KRAS-Gly12Cys (G12C), mutant KRAS-Gly12Asp (G12D), or mutant KRAS-Gly12Val (G12V). (D) KEGG analysis of the biological pathways enriched for significantly dysregulated genes in cell lines with the KRAS-G12D mutation compared to other substitutions of the KRAS gene. (E-F) The conjoint analysis (E) and heatmap plot (F) of significantly dysregulated genes in LUAD samples and cell lines with KRAS-G12D mutation compared with other KRAS mutations. (G) Cross-correlogram based on Pearson's r values among PD-L1, CXCL10, CXCL11 and the significantly dysregulated genes in LUAD samples with KRAS mutations. (H) Cross-correlogram based on Pearson's r values among HMGA2 level and infiltration of six tumor-infiltrated immune cells in LUAD samples with KRAS mutations via TIMER. (I) IHC analysis of correlations among levels of PD-L1, CXCL10, CXCL11, and HMGA2 and infiltration of CD8⁺ T cells in LUAD samples with KRAS mutations. (J) IHC analysis of HMGA2 protein level in LUAD samples with KRAS mutation. (K) Western blotting analysis of protein levels of PD-L1, CXCL10, CXCL11, and HMGA2 in Beas-2B cells with KRAS mutation. (L) Western blotting analysis of protein levels of PD-L1, CXCL10 and CXCL11 in control cells or HMGA2-overexpressing Beas-2B-G12D, SK-LU-1, and A427 cells. Abbreviations: KO, knockout; NC, normal control; G12D, samples with KRAS-G12D mutation; non-G12D, samples without KRAS-G12D mutation; IHC, immunohistochemistry; H-VEC, cells transfected with empty vector; H-OE, cells transfected with vector coding for HMGA2.

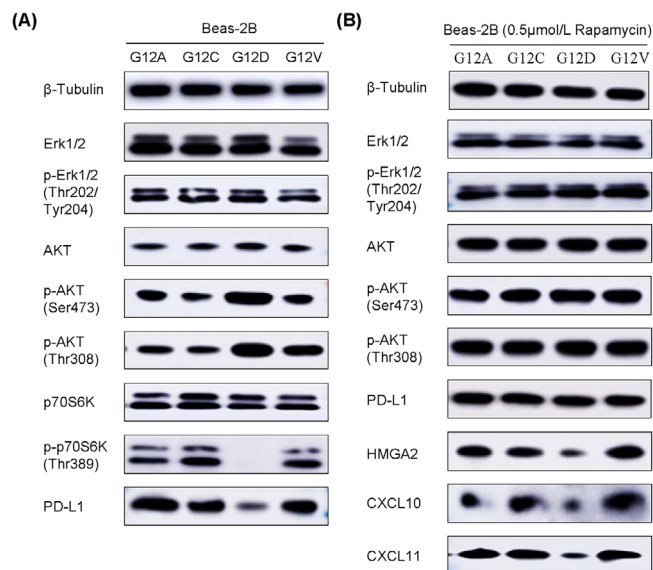


FIGURE 5 KRAS-G12D mutation suppressed PD-L1 protein level via the P70S6K/PI3K/AKT axis. (A) Western blotting analysis of PD-L1 and kinase signaling pathways in Beas-2B cells with KRAS mutation. (B) Western blotting analysis of protein levels of PD-L1, CXCL10, CXCL11, and HMGA2 and kinase signaling pathway in cell lines with KRAS mutation after treatment with the mTOR inhibitor rapamycin (0.5 $\mu\text{mol/L}$) for 24 h. Abbreviations: G12A, Beas-2B cells stably transfected with vector coding for mutant KRAS-Gly12Ala (G12A); G12C, Beas-2B cells stably transfected with vector coding for mutant KRAS-Gly12Cys (G12C); G12D, Beas-2B cells stably transfected with vector coding for mutant KRAS-Gly12Asp (G12D); G12V, Beas-2B cells stably transfected with vector coding for mutant KRAS-Gly12Val (G12V).

protein or mRNA levels of HMGA2, CXCL10 and CXCL11 as well as levels of secreted CXCL10 and CXCL11 in Beas-2B cells expressing the G12D point mutation remained lowest among the KRAS-transfected Beas-2B cell lines (Figure 5B, Supplementary Figure S7B-F).

3.5 | Paclitaxel-based chemotherapy recruited CD8⁺ T cells by upregulating CXCL10 and CXCL11 via HMGA2

A recent study showed that chemotherapy can induce tumor cells to secrete CXCL11 via the upregulation of HMGB1 level, thereby promoting the infiltration of CD8⁺ T cells in NSCLC [46]. Given that HMGA2 and HMGB1 are HMG family proteins, and paclitaxel is approved for the treatment of NSCLC, including LUAD and LUSC [47, 48], three cell lines harboring KRAS-G12D mutations (Beas-2B-G12D, SK-LU-1, A427) were treated with paclitaxel-based chemotherapy, and the effect on the levels of HMGA2, CXCL10 and CXCL11 were evaluated. The results revealed that paclitaxel increased the expression levels of HMGA2,

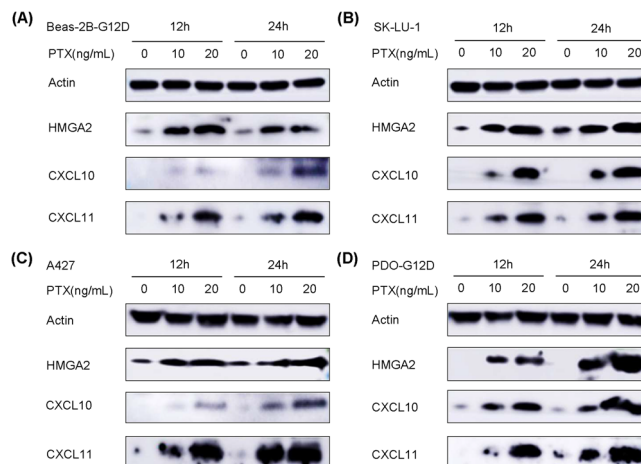
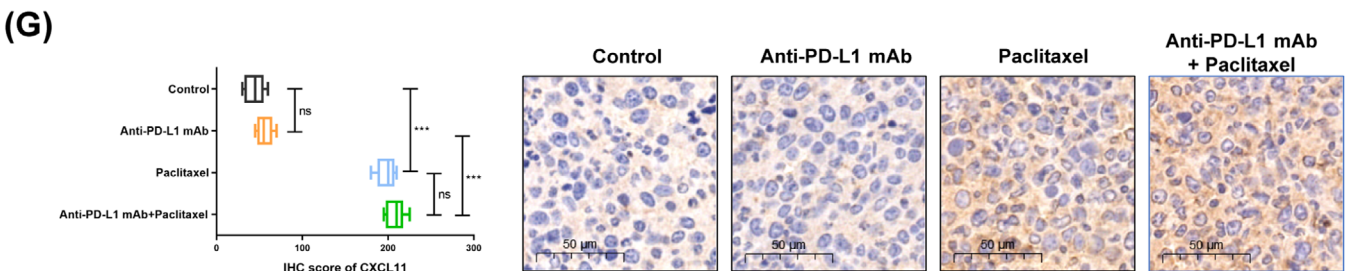
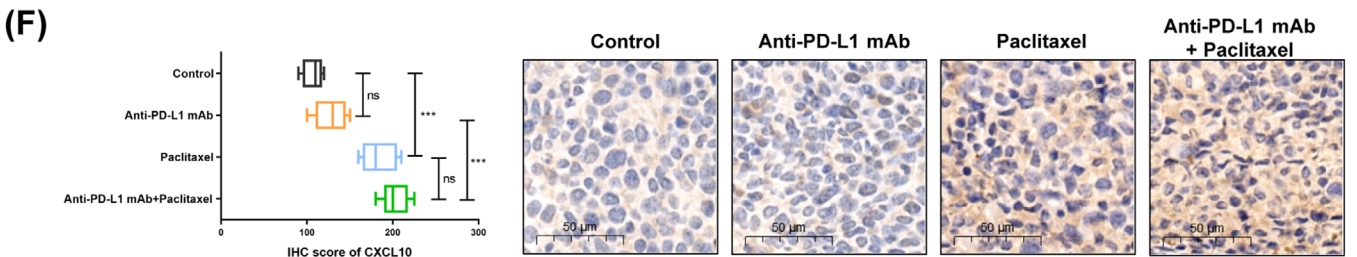
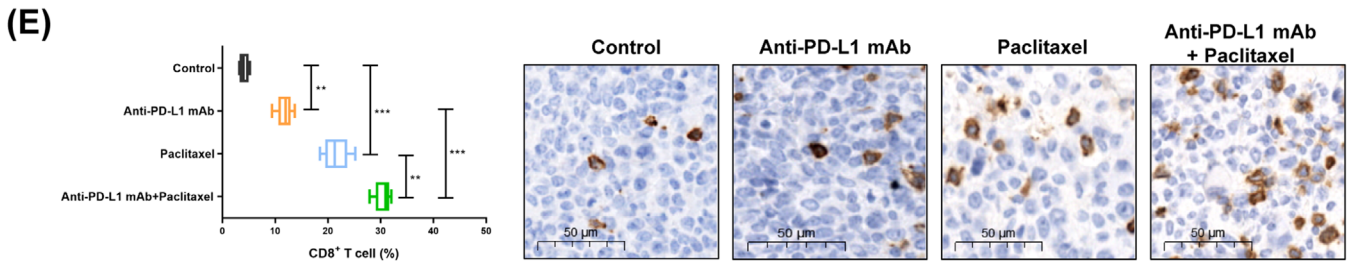
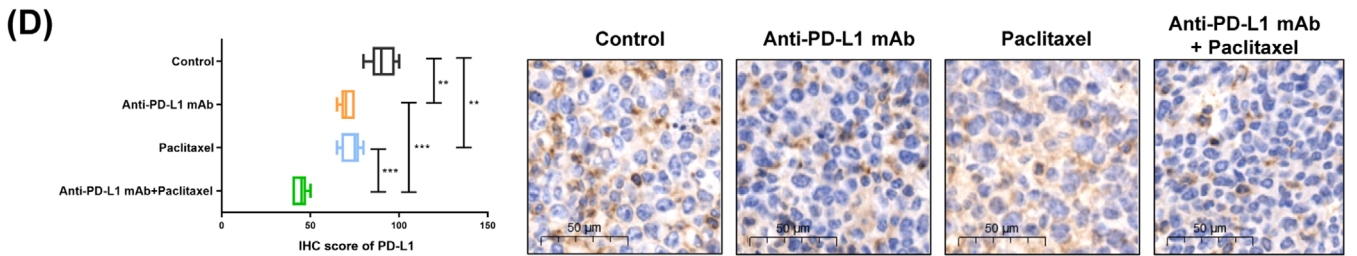
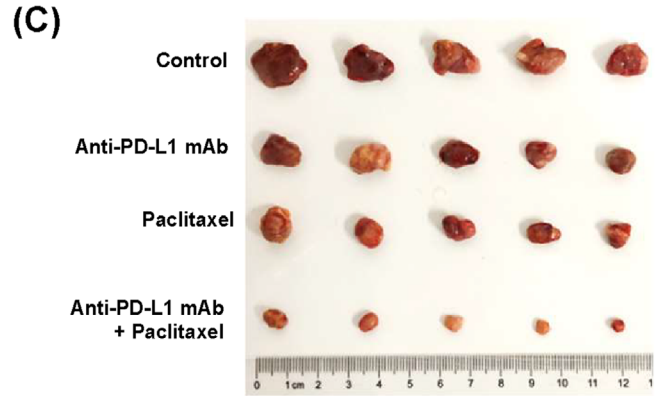
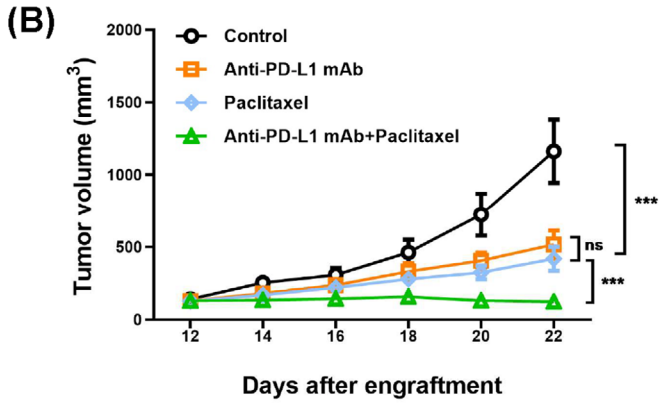
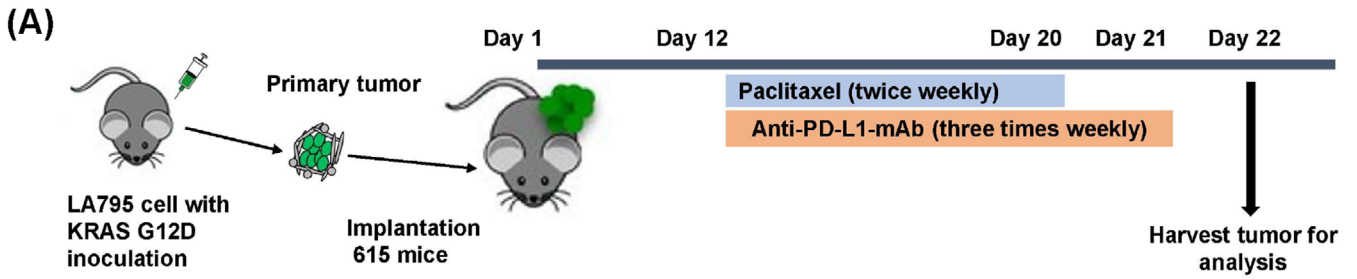


FIGURE 6 Paclitaxel upregulated protein levels of chemokines CXCL10/CXCL11 via HMGA2. Western blotting analysis of protein levels of CXCL10, CXCL11 and HMGA2 in Beas-2B-G12D (A), SK-LU-1 (B), A427 (C) cells, and KRAS-G12D-mutant organoids (D) treated with paclitaxel. Abbreviations: Beas-2B-G12D, Beas-2B cells stably transfected with vector coding for mutant KRAS-Gly12Asp (G12D); PTX: paclitaxel; PDO-G12D, a patient-derived organoid model with KRAS-G12D mutation.

CXCL10 and CXCL11 in a concentration-dependent manner (Figure 6A-C, Supplementary Figure S8). In addition, a patient-derived organoid (PDO) model with KRAS-G12D mutation was constructed and treated with paclitaxel (Supplementary Figure S9). Consistent with the results of the cells, the levels of HMGA2, CXCL10, and CXCL11 in PDO model with KRAS-G12D mutation were also upregulated in a concentration-dependent manner (Figure 6D, Supplementary Figure S10).

3.6 | Chemo-immunotherapy as a treatment for KRAS-G12D-mutant NSCLC with primary resistance to ICI monotherapy

As chemotherapy could ameliorate the immunosuppressive TIME induced by the KRAS-G12D mutation by recruiting CD8⁺ T cells via upregulation of HMGA2, CXCL10 and CXCL11, we hypothesized that combined treatment with ICIs and chemotherapy would be a better option for NSCLC with KRAS-G12D mutation. A mouse model with KRAS-G12D mutation was established to receive anti-PD-L1 mAb or paclitaxel as a monotherapy or combined therapy (Figure 7A). Compared to the other groups, anti-PD-L1 mAb with paclitaxel remarkably suppressed tumor growth in the mice ($P < 0.001$; Figure 7B-C). IHC analysis showed that combined treatment significantly reduced PD-L1 protein levels, increased the protein levels of CXCL10 and



CXCL11, and promoted the infiltration of CD8⁺ T cells (Figure 7D-G). Although the infiltration of CD8⁺ T cells and the expression of CXCL10 and CXCL11 increased after the intervention of paclitaxel, more abundant CD8⁺ T cells and more levels of CXCL10 and CXCL11 were observed in the combined treatment group (Figure 7E-G).

The above-mentioned mouse data paved the way for combination treatment with ICIs and chemotherapy as a rational, promising therapy to improve the immunosuppressive state and enhance the infiltration of CD8⁺ T cells in patients with *KRAS*-G12D-mutant NSCLC. Therefore, we retrospectively collected the clinical information of patients with NSCLC harboring *KRAS*-G12D mutation after ICI monotherapy or chemo-immunotherapy (Supplementary Table S6). In total, 11 patients were included to undertake treatment efficacy evaluations. Three (27.3%) patients received anti-PD-1 agent monotherapy, and 8 (72.7%) received chemo-immunotherapy. Three (27.3%) patients were identified with partial response, 3 (27.3%) patients with stable disease, and 5 (45.5%) with progressive disease (PD). Because the follow-up time of 2 (18.2%) patients was less than 6 months, 5 (45.5%) patients were determined to have DCB, and 4 (36.4%) to have non-DCB (PFS ≤ 6 months). Although there was no statistical difference, the proportion of PD and non-DCB was lower in the chemo-immunotherapy group compared to the ICI monotherapy group (Figure 8A-B). At the time of survival analysis, patients with NSCLC could obtain more benefit from chemo-immunotherapy with respect to PFS; however, there were no significant difference because of the small sample size ($P = 0.362$; Figure 8C). Of note, patients with *KRAS*-G12D-mutant NSCLC receiving chemo-immunotherapy had better overall survival (OS) than those with ICI monotherapy ($P = 0.002$; Figure 8D).

4 | DISCUSSION

Although the successful application of small-molecule inhibitors targeting *KRAS*-G12C mutations in clinical trials has demonstrated that *KRAS* mutations are not “undruggable”, these drugs are not yet ready to enter clinical practice. Therefore, ICIs targeting the PD-1/PD-L1 axis, according to current guidelines, remains the optimal treatment for these patients [13, 49]. However, in contrast to

other variants of *KRAS* mutations, our study found that the *KRAS*-G12D mutation drove immunosuppression and the primary resistance of immunotherapy against PD-1/PD-L1 by downregulating PD-L1 level and infiltration of CD8⁺ TILs in NSCLC.

Consistent with others, our study also proved that *KRAS* mutations were positively correlated with CD8⁺ TILs, PD-L1 level, and TMB, thereby resulting in an inflammatory TIME with adaptive immune resistance that is associated with a superior response to ICIs [17, 50]. However, NSCLC with *KRAS* mutation is a heterogeneous disease with different molecular characteristics, including distinct point variations and tumor-associated co-mutations [49]. Recent clinical studies have demonstrated that *KRAS* mutations do not perfectly guide immunotherapy in advanced NSCLC. First, emerging data indicate improved efficacy in patients with *KRAS* mutations and co-mutant *TP53*, and reduced efficacy in patients with *KRAS* mutations and co-mutant *STK11/LKBI*, *KEAP1/NFE2L2* or *SMARCA4* [51w-55]. Second, although some previous studies have found that there are no significant differences in clinical benefit among patients with NSCLC harboring different variant statuses of the *KRAS* oncogene, the KEYNOTE042 study reported that the *KRAS*-G12C mutant subgroup receiving pembrolizumab monotherapy had a higher objective response rate, as well as longer PFS and OS, than other subgroups [56-60]. Interestingly, in an online clinical cohort of 74 patients with NSCLC, we found that *KRAS*-G12D mutations derived less benefit from ICI monotherapy. To confirm this finding, a co-culture system evaluating the tumoricidal activity of CD8⁺ T cells cocultured with *KRAS*-mutant tumor cells, as well as a LUAD mouse model with different *KRAS* oncogene substitutions, was established.

Previous studies have demonstrated that the predictive biomarkers of clinical benefit of NSCLC treated with ICIs include the TIME (PD-L1 level, CD8⁺ TILs, and other immune cells), genetic alterations (TMB, the loss and gain of activated mutations), and the host immune system [61, 62]. Consistent with the results of a recent publication [23], our study also found that patients with *KRAS*-G12D-mutant NSCLC tend to have lower TMB via *in silico* analysis of the clinical cohort and the TCGA database.

In addition, our study showed that the *KRAS*-G12D mutation was correlated with low level of PD-L1 and low

FIGURE 7 PD-L1 blockade combined with paclitaxel elicited synergistic anti-tumor immune responses in the *KRAS*^{G12D}-mutant mouse model. (A) Scheme for constructing a mouse model with the *KRAS*-G12D mutation and dosing schedule. (B) The mice bearing LA795 cells with *KRAS*-G12D mutation ($n = 5$) received treatment with paclitaxel and/or anti-PD-L1 monoclonal antibody (mAb). Control mice were treated with vehicle control. The combination of anti-PD-L1 mAb and paclitaxel significantly weakened tumor growth compared to the other treated group in *KRAS*^{G12D}-mutant mice. (C) Representative images of tumor nodules in each treated group from B.(D-G) The distributions of IHC score of PD-L1 (D), CD8⁺ T cell (E), IHC scores of CXCL10 (F) and CXCL11 (G) in each treated group, as well as the representative IHC images. *, $P > 0.05$; **, $P < 0.01$; ***, $P < 0.001$; ns, not significant. Abbreviations: IHC, immunohistochemistry.

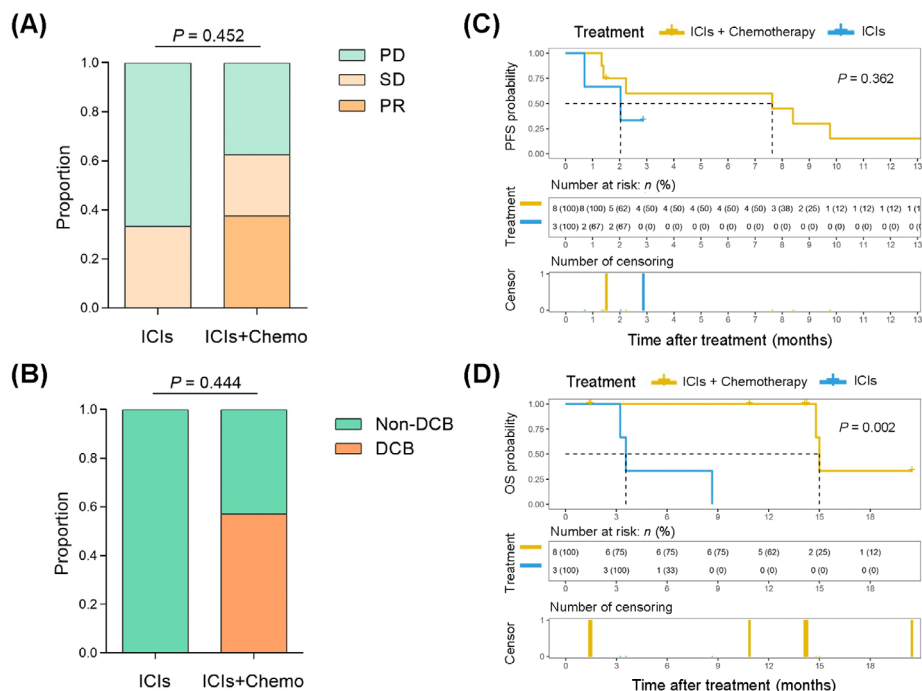


FIGURE 8 Patients with *KRAS*-G12D mutations showed favorable clinical benefits from chemo-immunotherapy. (A-B) Boxplots evaluating tumor response (A) and durable clinical benefit (B) of patients with NSCLC harboring *KRAS*-G12D mutations after PD-1/PD-L1 inhibitor monotherapy or chemo-immunotherapy. (C-D) Kaplan-Meier survival curves of patients with NSCLC harboring *KRAS*-G12D mutations after initiation of PD-1/PD-L1 blockade monotherapy treatment or chemo-immunotherapy concerning progression-free survival (C) and overall survival (D). Abbreviations: ICIs, immune checkpoint inhibitors; ICIs+Chemo, chemo-immunotherapy; PR, patients with partial response; SD, patients with stable disease; PD, patients with progressive disease; DCB, patients with durable clinical benefit; non-DCB, patients with no durable clinical benefit; PFS, progression-free survival; OS, overall survival.

infiltration of CD8⁺ TILs, inducing an immunosuppressive TIME. Several studies also analyzed the association between *KRAS* oncogene substitutions and PD-L1 level in tumor samples with NSCLC. Arbour *et al.* [57] stated that PD-L1 level was higher in patients with *KRAS*-G12C-mutant NSCLC compared to those with non-G12C mutations. Another study showed that *KRAS*-G12V mutation promoted PD-L1 level via the transcription of growth factor beta (TGF- β)/epithelial-to-mesenchymal transition (EMT) pathway in NSCLC [30]. These conclusions do not contradict our finding that the *KRAS*-G12D mutation was negatively correlated with PD-L1 level. Although a previous study reported that *KRAS* mutation increased PD-L1 level via the MEK-ERK pathway [44], our study found that *KRAS*-G12D mutations not only activated the MEK-ERK signaling pathway but also suppressed PD-L1 level via the P70S6K/PI3K/AKT axis. These mechanisms explain why PD-L1 level of NSCLC with *KRAS*-G12D mutation was lower than other *KRAS* substitutions.

Of note, our study proposed that *KRAS*-G12D mutation suppressed the secretion of chemokines CXCL10/CXCL11 in TIME by downregulating the HMG2 signaling, leading to a decrease in CD8⁺ TILs, which in turn built up a suppressive TIME that is primarily resistant to anti-

PD-1/PD-L1 immunotherapy in NSCLC. In addition, some studies have reported the role of *KRAS*-G12D mutation, a common oncogene driver in these tumors, in the construction of TIME in pancreatic and colorectal cancers. Cheng *et al.* [63] found that *KRAS*-G12D mutation promoted the conversion of regulatory T cells by activating the MEK/ERK pathway, resulting in an immunosuppressive TIME in pancreatic cancer. Liao *et al.* [64] reported that *KRAS*-G12D mutation increased the infiltration of bone marrow-derived suppressor cells via the IRF2-CXCL3-CXCR2 axis, therapy leading to an immunosuppressive TIME that avoided T cell killing and caused resistance to immunotherapy in colorectal cancer.

According to current guidelines, chemo-immunotherapy is recommended as the first-line treatment for advanced NSCLC [65, 66]. However, from recent clinical data, ICIs combined with chemotherapy did not always increase the clinical benefit compared to ICIs alone in patients with *KRAS*-mutant NSCLC. Sun *et al.* [67] reported that among patients with *KRAS* mutations and PD-L1 level of 50% or greater, there was no difference in OS between those receiving ICI monotherapy and those receiving chemo-immunotherapy. Our previous study also demonstrated that anti-PD-L1 drugs combined

with docetaxel did not extend the anti-tumor response in a mouse model with the *KRAS*-G12C mutation [17]. Interestingly, in the current research, ICI in combination with chemotherapy was shown to be more effective than ICI monotherapy in patients with *KRAS*-G12D-mutant NSCLC. We found that paclitaxel-based chemotherapy could recruit CD8⁺ T cells by upregulation of levels of CXCL10 and CXCL11 via the HMGA2 signaling, thereby meliorating the immunosuppressive TIME induced by the *KRAS*-G12D mutation. However, *KRAS*-mutant tumors with non-G12D mutations generally had high expression of PD-L1 and abundant TIL infiltration, suggesting a greater sensitivity to ICIs. Thus, when ICIs were combined with chemotherapy, the TIME was not effectively improved, the infiltration of CD8⁺ T cells was not increased, and additional clinical benefits were not observed in *KRAS*-mutant tumors with non-G12D mutations. Together, these results suggest a potential mechanism for the vulnerability of NSCLC with *KRAS*-G12D mutations to chemo-immunotherapy. However, the limitations of the present study should be recognized. For example, these findings were only verified by a preclinical mouse model and limited clinical data. Further validation should be performed in large prospective clinical trials in the future.

5 | CONCLUSIONS

In conclusion, our study elucidated the molecular mechanism by which *KRAS*-G12D mutation drives immunosuppression and the primary resistance of immunotherapy against PD-1/PD-L1 in NSCLC. Moreover, we propose that a combination of ICIs and chemotherapy may be more effective in patients with *KRAS*-G12D-mutant NSCLC.

DECLARATIONS

ACKNOWLEDGEMENTS

Not applicable.

COMPETING INTERESTS

The authors declare that they have no competing interests.

AUTHOR CONTRIBUTIONS

Chengming Liu: project design, cell experiment, data curation, formal analysis, and writing-original draft preparation. Sufei Zheng, Zhanyu Wang, Sihui Wang, and Xinfeng Wang: mouse experiment and data analysis. Lu Yang, Haiyan Xu, and Zheng Cao: data curation and data analysis.

Xiaoli Feng, Qi Xue, and Yan Wang: project supervision and formal analysis. Jie He, Yan Wang, and Nan Sun: project administration, supervision, writing-reviewing and

editing and funding acquisition. All authors read and approved the final manuscript.

ETHICS APPROVAL AND CONSENT TO PARTICIPATE

The human study was approved by the Ethics Committee of Cancer Hospital and Institute, Chinese Academy of Medical Sciences (permit number: #20/242-2438). The tissue samples were obtained with written informed consent from each patient. The animal study was carried out in compliance with the guidance suggestion of Animal Care Committee of Cancer Hospital and Institute, Chinese Academy of Medical Sciences (permit number: #NCC2020A163).

CONSENT FOR PUBLICATION

Not applicable.

AVAILABILITY OF DATA AND MATERIALS

The datasets used and/or analyzed in the present study can be obtained from the corresponding authors as reasonably required.

ORCID

Qi Xue  <https://orcid.org/0000-0002-5086-4654>

Yan Wang  <https://orcid.org/0000-0002-1743-6383>

Jie He  <https://orcid.org/0000-0002-0285-5403>

REFERENCES

1. Siegel RL, Miller KD, Jemal A. Cancer statistics. *CA Cancer J Clin.* 2019;69(1):7-34.
2. Qiu H, Cao S, Xu R. Cancer incidence, mortality, and burden in China: a time-trend analysis and comparison with the United States and United Kingdom based on the global epidemiological data released in 2020. *Cancer Commun (Lond).* 2021;41(10):1037-48.
3. Zhang S, Sun K, Zheng R, Zeng H, Wang S, Chen R, et al. Cancer incidence and mortality in China. 2015. *Journal of the National Cancer Center.* 2020.
4. Travis WD, Brambilla E, Nicholson AG, Yatabe Y, Austin JHM, Beasley MB, et al. The 2015 World Health Organization Classification of Lung Tumors: Impact of Genetic, Clinical and Radiologic Advances Since the 2004 Classification. *J Thorac Oncol.* 2015;10(9):1243-60.
5. Duma N, Santana-Davila R, Molina JR. Non-Small Cell Lung Cancer: Epidemiology, Screening, Diagnosis, and Treatment. *Mayo Clin Proc.* 2019;94(8):1623-40.
6. Reck M, Rabe KF. Precision Diagnosis and Treatment for Advanced Non-Small-Cell Lung Cancer. *N Engl J Med.* 2017;377(9):849-61.
7. Rodak O, Peris-Díaz MD, Olbromski M, Podhorska-Okołów M, Dziągiel P. Current Landscape of Non-Small Cell Lung Cancer: Epidemiology, Histological Classification, Targeted Therapies, and Immunotherapy. *Cancers (Basel).* 2021;13(18).

8. Zhou C, Wu YL, Chen G, Feng J, Liu XQ, Wang C, et al. Erlotinib versus chemotherapy as first-line treatment for patients with advanced EGFR mutation-positive non-small-cell lung cancer (OPTIMAL, CTONG-0802): a multicentre, open-label, randomised, phase 3 study. *Lancet Oncol.* 2011;12(8):735-42.
9. Solomon BJ, Mok T, Kim DW, Wu YL, Nakagawa K, Mekhail T, et al. First-line crizotinib versus chemotherapy in ALK-positive lung cancer. *N Engl J Med.* 2014;371(23):2167-77.
10. Ramalingam SS, Yang JC, Lee CK, Kurata T, Kim DW, John T, et al. Osimertinib As First-Line Treatment of EGFR Mutation-Positive Advanced Non-Small-Cell Lung Cancer. *J Clin Oncol.* 2018;36(9):841-9.
11. Hong DS, Fakih MG, Strickler JH, Desai J, Durm GA, Shapiro GI, et al. KRAS(G12C) Inhibition with Sotorasib in Advanced Solid Tumors. *N Engl J Med.* 2020;383(13):1207-17.
12. Hallin J, Engstrom LD, Hargis L, Calinisan A, Aranda R, Briere DM, et al. The KRAS(G12C) Inhibitor MRTX849 Provides Insight toward Therapeutic Susceptibility of KRAS-Mutant Cancers in Mouse Models and Patients. *Cancer Discov.* 2020;10(1):54-71.
13. Reck M, Carbone DP, Garassino M, Barlesi F. Targeting KRAS in non-small cell lung cancer: recent progress and new approaches. *Ann Oncol.* 2021.
14. Ma L, Diao B, Huang Z, Wang B, Yu J, Meng X. The efficacy and possible mechanisms of immune checkpoint inhibitors in treating non-small cell lung cancer patients with epidermal growth factor receptor mutation. *Cancer Commun (Lond).* 2021;41(12):1314-30.
15. Ribas A, Wolchok JD. Cancer immunotherapy using checkpoint blockade. *Science.* 2018;359(6382):1350-5.
16. Lee CK, Man J, Lord S, Cooper W, Links M, GebSKI V, et al. Clinical and Molecular Characteristics Associated With Survival Among Patients Treated With Checkpoint Inhibitors for Advanced Non-Small Cell Lung Carcinoma: A Systematic Review and Meta-analysis. *JAMA Oncol.* 2018;4(2):210-6.
17. Liu C, Zheng S, Jin R, Wang X, Wang F, Zang R, et al. The superior efficacy of anti-PD-1/PD-L1 immunotherapy in KRAS-mutant non-small cell lung cancer that correlates with an inflammatory phenotype and increased immunogenicity. *Cancer Lett.* 2020;470:95-105.
18. Jordan EJ, Kim HR, Arcila ME, Barron D, Chakravarty D, Gao J, et al. Prospective Comprehensive Molecular Characterization of Lung Adenocarcinomas for Efficient Patient Matching to Approved and Emerging Therapies. *Cancer Discov.* 2017;7(6):596-609.
19. Dearden S, Stevens J, Wu YL, Blowers D. Mutation incidence and coincidence in non small-cell lung cancer: meta-analyses by ethnicity and histology (mutMap). *Ann Oncol.* 2013;24(9):2371-6.
20. Osta BEE, Behera M, Kim S, Berry LD, Sica G, Pillai RN, et al. Characteristics and outcomes of patients (pts) with metastatic KRAS mutant lung adenocarcinomas: Lung Cancer Mutation Consortium (LCMC) database. *J Clin Oncol.* 2017;35(15_suppl):9021-.
21. Wood K, Hensing T, Malik R, Sargia R. Prognostic and Predictive Value in KRAS in Non-Small-Cell Lung Cancer: A Review. *JAMA Oncol.* 2016;2(6):805-12.
22. Jia Y, Jiang T, Li X, Zhao C, Zhang L, Zhao S, et al. Characterization of distinct types of KRAS mutation and its impact on first-line platinum-based chemotherapy in Chinese patients with advanced non-small cell lung cancer. *Oncol Lett.* 2017;14(6):6525-32.
23. Gao G, Liao W, Ma Q, Zhang B, Chen Y, Wang Y. KRAS G12D mutation predicts lower TMB and drives immune suppression in lung adenocarcinoma. *Lung Cancer.* 2020;149:41-5.
24. El Osta B, Behera M, Kim S, Berry LD, Sica G, Pillai RN, et al. Characteristics and Outcomes of Patients With Metastatic KRAS-Mutant Lung Adenocarcinomas: The Lung Cancer Mutation Consortium Experience. *J Thorac Oncol.* 2019;14(5):876-89.
25. Garassino MC, Marabese M, Rusconi P, Rulli E, Martelli O, Farina G, et al. Different types of K-Ras mutations could affect drug sensitivity and tumour behaviour in non-small-cell lung cancer. *Ann Oncol.* 2011;22(1):235-7.
26. Lei L, Wang WX, Yu ZY, Liang XB, Pan WW, Chen HF, et al. A Real-World Study in Advanced Non-Small Cell Lung Cancer with KRAS Mutations. *Transl Oncol.* 2020;13(2):329-35.
27. Ihle NT, Byers LA, Kim ES, Saintigny P, Lee JJ, Blumenschein GR, et al. Effect of KRAS oncogene substitutions on protein behavior: implications for signaling and clinical outcome. *J Natl Cancer Inst.* 2012;104(3):228-39.
28. Al-Mulla F, Milner-White EJ, Going JJ, Birnie GD. Structural differences between valine-12 and aspartate-12 Ras proteins may modify carcinoma aggression. *J Pathol.* 1999;187(4):433-8.
29. Falk AT, Yazbeck N, Guibert N, Chamorey E, Paquet A, Ribeyre L, et al. Effect of mutant variants of the KRAS gene on PD-L1 expression and on the immune microenvironment and association with clinical outcome in lung adenocarcinoma patients. *Lung Cancer.* 2018;121:70-5.
30. Pan LN, Ma YF, Li Z, Hu JA, Xu ZH. KRAS G12V mutation upregulates PD-L1 expression via TGF- β /EMT signaling pathway in human non-small-cell lung cancer. *Cell Biol Int.* 2021;45(4):795-803.
31. Rizvi H, Sanchez-Vega F, La K, Chatila W, Jonsson P, Halpenny D, et al. Molecular Determinants of Response to Anti-Programmed Cell Death (PD)-1 and Anti-Programmed Death-Ligand 1 (PD-L1) Blockade in Patients With Non-Small-Cell Lung Cancer Profiled With Targeted Next-Generation Sequencing. *J Clin Oncol.* 2018;36(7):633-41.
32. Lei Y, Lu Z, Huang J, Zang R, Che Y, Mao S, et al. The membrane-bound and soluble form of melanotransferrin function independently in the diagnosis and targeted therapy of lung cancer. *Cell Death Dis.* 2020;11(10):933.
33. Liu C, Wang S, Zheng S, Wang X, Huang J, Lei Y, et al. A novel recurrence-associated metabolic prognostic model for risk stratification and therapeutic response prediction in patients with stage I lung adenocarcinoma. *Cancer Biol Med.* 2021;18(3):734-49.
34. Liu C, Zheng S, Wang S, Wang X, Feng X, Sun N, et al. Development and external validation of a composite immune-clinical prognostic model associated with EGFR mutation in East-Asian patients with lung adenocarcinoma. *Therapeutic Advances in Medical Oncology.* 2021;13:17588359211006949.
35. Chuai G, Ma H, Yan J, Chen M, Hong N, Xue D, et al. Deep-CRISPR: optimized CRISPR guide RNA design by deep learning. *Genome Biol.* 2018;19(1):80.
36. Lu Z, Zheng S, Liu C, Wang X, Zhang G, Wang F, et al. S100A7 as a potential diagnostic and prognostic biomarker of esophageal squamous cell carcinoma promotes M2 macrophage infiltration and angiogenesis. *Clin Transl Med.* 2021;11(7):e459.

37. Love MI, Huber W, Anders S. Moderated estimation of fold change and dispersion for RNA-seq data with DESeq2. *Genome Biol.* 2014;15(12):550.
38. Cesano A. nCounter((R)) PanCancer Immune Profiling Panel (NanoString Technologies, Inc., Seattle, WA). *J Immunother Cancer.* 2015;3:42.
39. Franks JM, Cai G, Whitfield ML. Feature specific quantile normalization enables cross-platform classification of molecular subtypes using gene expression data. *Bioinformatics.* 2018;34(11):1868-74.
40. Li H, Wang J, Yi Z, Li C, Wang H, Zhang J, et al. CDK12 inhibition enhances sensitivity of HER2+ breast cancers to HER2-tyrosine kinase inhibitor via suppressing PI3K/AKT. *Eur J Cancer.* 2021;145:92-108.
41. Jin R, Liu C, Zheng S, Wang X, Feng X, Li H, et al. Molecular heterogeneity of anti-PD-1/PD-L1 immunotherapy efficacy is correlated with tumor immune microenvironment in East Asian patients with non-small cell lung cancer. *Cancer Biol Med.* 2020;17(3):768-81.
42. Sanmamed MF, Chen L. A Paradigm Shift in Cancer Immunotherapy: From Enhancement to Normalization. *Cell.* 2018;175(2):313-26.
43. Tokunaga R, Zhang W, Naseem M, Puccini A, Berger MD, Soni S, et al. CXCL9, CXCL10, CXCL11/CXCR3 axis for immune activation - A target for novel cancer therapy. *Cancer Treat Rev.* 2018;63:40-7.
44. Coelho MA, de Carne Trecesson S, Rana S, Zecchin D, Moore C, Molina-Arcas M, et al. Oncogenic RAS Signaling Promotes Tumor Immunoresistance by Stabilizing PD-L1 mRNA. *Immunity.* 2017;47(6):1083-99.e6.
45. Dunlop EA, Tee AR. Mammalian target of rapamycin complex 1: signalling inputs, substrates and feedback mechanisms. *Cell Signal.* 2009;21(6):827-35.
46. Gao Q, Wang S, Chen X, Cheng S, Zhang Z, Li F, et al. Cancer-cell-secreted CXCL11 promoted CD8(+) T cells infiltration through docetaxel-induced-release of HMGB1 in NSCLC. *J Immunother Cancer.* 2019;7(1):42.
47. Strichman-Almashanu LZ, Bustin M, Landsman D. Retroposed copies of the HMG genes: a window to genome dynamics. *Genome Res.* 2003;13(5):800-12.
48. Adrianzen Herrera D, Ashai N, Perez-Soler R, Cheng H. Nanoparticle albumin bound-paclitaxel for treatment of advanced non-small cell lung cancer: an evaluation of the clinical evidence. *Expert Opin Pharmacother.* 2019;20(1):95-102.
49. Moore AR, Rosenberg SC, McCormick F, Malek S. RAS-targeted therapies: is the undruggable drugged? *Nat Rev Drug Discov.* 2020;19(8):533-52.
50. Adderley H, Blackhall FH, Lindsay CR. KRAS-mutant non-small cell lung cancer: Converging small molecules and immune checkpoint inhibition. *EBioMedicine.* 2019;41:711-6.
51. Arbour KC, Jordan E, Kim HR, Dienstag J, Yu HA, Sanchez-Vega F, et al. Effects of Co-occurring Genomic Alterations on Outcomes in Patients with KRAS-Mutant Non-Small Cell Lung Cancer. *Clin Cancer Res.* 2018;24(2):334-40.
52. Davis AP, Cooper WA, Boyer M, Lee JH, Pavlakis N, Kao SC. Efficacy of immunotherapy in KRAS-mutant non-small-cell lung cancer with comutations. *Immunotherapy.* 2021.
53. Skoulidis F, Goldberg ME, Greenawalt DM, Hellmann MD, Awad MM, Gainor JF, et al. STK11/LKB1 Mutations and PD-1 Inhibitor Resistance in KRAS-Mutant Lung Adenocarcinoma. *Cancer Discov.* 2018;8(7):822-35.
54. Koyama S, Akbay EA, Li YY, Aref AR, Skoulidis F, Herter-Sprie GS, et al. STK11/LKB1 Deficiency Promotes Neutrophil Recruitment and Proinflammatory Cytokine Production to Suppress T-cell Activity in the Lung Tumor Microenvironment. *Cancer Res.* 2016;76(5):999-1008.
55. Alessi JV, Ricciuti B, Spurr LF, Gupta H, Li YY, Glass C, et al. SMARCA4 and Other SWItch/Sucrose NonFermentable Family Genomic Alterations in NSCLC: Clinicopathologic Characteristics and Outcomes to Immune Checkpoint Inhibition. *J Thorac Oncol.* 2021;16(7):1176-87.
56. Negrao MV, Skoulidis F, Montesion M, Schulze K, Bara I, Shen V, et al. Oncogene-specific differences in tumor mutational burden, PD-L1 expression, and outcomes from immunotherapy in non-small cell lung cancer. *J Immunother Cancer.* 2021;9(8).
57. Arbour KC, Rizvi H, Plodkowski AJ, Hellmann MD, Knezevic A, Heller G, et al. Treatment Outcomes and Clinical Characteristics of Patients with KRAS-G12C Mutant Non-Small Cell Lung Cancer. *Clin Cancer Res.* 2021.
58. Jeanson A, Tomasini P, Souquet-Bressand M, Brandone N, Boucekine M, Grangeon M, et al. Brief report: efficacy of immune checkpoint inhibitors in KRAS-mutant Non-small cell lung cancer (NSCLC). *J Thorac Oncol.* 2019.
59. Kartolo A, Feilotter H, Hopman W, Fung AS, Robinson A. A single institution study evaluating outcomes of PD-L1 high KRAS-mutant advanced non-small cell lung cancer (NSCLC) patients treated with first line immune checkpoint inhibitors. *Cancer Treat Res Commun.* 2021;27:100330.
60. Mok TSK, Wu YL, Kudaba I, Kowalski DM, Cho BC, Turna HZ, et al. Pembrolizumab versus chemotherapy for previously untreated, PD-L1-expressing, locally advanced or metastatic non-small-cell lung cancer (KEYNOTE-042): a randomised, open-label, controlled, phase 3 trial. *Lancet.* 2019;393(10183):1819-30.
61. Prelaj A, Tay R, Ferrara R, Chaput N, Besse B, Califano R. Predictive biomarkers of response for immune checkpoint inhibitors in non-small-cell lung cancer. *Eur J Cancer.* 2019;106:144-59.
62. Bodor JN, Boumber Y, Borghaei H. Biomarkers for immune checkpoint inhibition in non-small cell lung cancer (NSCLC). *Cancer.* 2020;126(2):260-70.
63. Cheng H, Fan K, Luo G, Fan Z, Yang C, Huang Q, et al. Kras(G12D) mutation contributes to regulatory T cell conversion through activation of the MEK/ERK pathway in pancreatic cancer. *Cancer Lett.* 2019;446:103-11.
64. Liao W, Overman MJ, Boutin AT, Shang X, Zhao D, Dey P, et al. KRAS-IRF2 Axis Drives Immune Suppression and Immune Therapy Resistance in Colorectal Cancer. *Cancer Cell.* 2019;35(4):559-72.e7.
65. Cheng Y, Li H, Zhang L, Liu JJ, Yang CL, Zhang S. Current and future drug combination strategies based on programmed death-1/programmed death-ligand 1 inhibitors in non-small cell lung cancer. *Chin Med J (Engl).* 2021;134(15):1780-8.
66. Lim SM, Hong MH, Kim HR. Immunotherapy for Non-small Cell Lung Cancer: Current Landscape and Future Perspectives. *Immune Netw.* 2020;20(1):e10.
67. Sun L, Hsu M, Cohen RB, Langer CJ, Mamtani R, Aggarwal C. Association Between KRAS Variant Status and Outcomes

With First-line Immune Checkpoint Inhibitor-Based Therapy in Patients With Advanced Non-Small-Cell Lung Cancer. *JAMA Oncol.* 2021;7(6):937-9.

SUPPORTING INFORMATION

Additional supporting information can be found online in the Supporting Information section at the end of this article.

How to cite this article: Liu C, Zheng S, Wang Z, Wang S, Wang X, Yang L, et al. *KRAS-G12D mutation drives immune suppression and the primary resistance of anti-PD-1/PD-L1 immunotherapy in non-small cell lung cancer.* 2022;42:828–847. <https://doi.org/10.1002/cac2.12327>